

BENCHMARKING OF QUANTUM AND CLASSICAL SDP RELAXATIONS FOR QUBO FORMULATIONS OF REAL-WORLD LOGISTICS PROBLEMS

BIRTE OSTERMANN¹, TAYLOR GARNOWSKI^{†,3}, FABIAN HENZE^{†,2}, VAIBHAVNATH JHA^{†,4}, ASRA DIA¹, FREDERIK FIAND⁴, DAVID GROSS², WENDELIN GROSS³, JULIAN NOWAK³, AND TIMO DE WOLFF^{*,1}

ABSTRACT. Quadratic unconstrained binary optimization problems (QUBOs) are intensively discussed in the realm of quantum computing and polynomial optimization. We provide a vast experimental study of semidefinite programming (SDP) relaxations of QUBOs using sums of squares methods and on Hamiltonian Updates. We test on QUBO reformulations of industry-based instances of the (open) vehicle routing problem and the (affinity-based) slotting problem – two common combinatorial optimization problems in logistics. Beyond comparing the performance of various methods and software, our results reaffirm that optimizing over non-generic, real-world instances provides additional challenges. In consequence, this study underscores recent developments towards structure exploitation and specialized solver development for the used methods and simultaneously shows that further research is necessary in this direction both on the classical and the quantum side.

1. INTRODUCTION

Problem Setting and Approach. In the last 25 years there has been plenty of development on solving nonlinear optimization problems and especially *(constrained) polynomial optimization problems (CPOPs)*

$$\begin{aligned} \min \quad & f(\mathbf{x}) \\ \text{subject to} \quad & h_1(\mathbf{x}) \geq 0, \dots, h_s(\mathbf{x}) \geq 0 \\ & \mathbf{x} \in \mathbb{R}^n, \end{aligned}$$

where the objective function $f(\mathbf{x}) \in \mathbb{R}[\mathbf{x}] = \mathbb{R}[x_1, \dots, x_n]$ and the constraints $h_1(\mathbf{x}), \dots, h_s(\mathbf{x}) \in \mathbb{R}[\mathbf{x}]$ are polynomial. A prominent subclass of CPOPs consists of *quadratic unconstrained binary optimization (QUBO)* problems, which are of the form

$$\min_{\mathbf{x} \in \{0,1\}^n} \mathbf{x}^T Q \mathbf{x},$$

for a given real symmetric $n \times n$ matrix $Q \in \mathbb{R}^{n \times n}$.

[†] THESE AUTHORS CONTRIBUTED EQUALLY TO THIS WORK.

* CORRESPONDING AUTHOR: t.de-wolff@tu-braunschweig.de

¹ INSTITUTE FOR ANALYSIS AND ALGEBRA, TU BRAUNSCHWEIG, GERMANY

² INSTITUTE FOR THEORETICAL PHYSICS, UNIVERSITY OF COLOGNE, GERMANY

³ 4FLOW SE, HALLERSTRASSE 1, 10587 BERLIN, GERMANY

⁴ GAMS SOFTWARE GMBH, PO BOX 4059, 50216 FRECHEN, GERMANY

2010 *Mathematics Subject Classification.* 81Q99, 90-05, 90C10 90C20, 90C22, 90C23.

Key words and phrases. Benchmarking, Quadratic Unconstrained Binary Optimization, Semidefinite Programming Relaxation, Quantum Algorithms, Hamiltonian Updates, Polynomial Optimization, Sums of Squares, Logistics.

QUBOs received a lot of attention not only because one can represent several real-world applications by them, but also due to their connection to approaches based on quantum computing. In fact, there exists a wide range of algorithms based on different classical and quantum (inspired) ansätze for solving QUBOs. Prominently, but not exclusively, these include

- (1) interpreting the QUBO as a CPOP, which is tackled via *sums of squares (SOS)*, or, on the dual side, *moment methods*. This approach leads to a hierarchy or lower bounds, known as *Lasserre’s hierarchy* [Las01, Par00]. Both the primal and the dual approach induce a *semidefinite program (SDP)*, which can classically be solved, e.g. using *interior point methods*.
- (2) similarly, from the quantum community perspective, interpreting the QUBO as in the Goemans-Williamson [GW95] approximation algorithm for the *maximum cut (MaxCut)* problem. This also results in an SDP (which coincides with the SDP in the first order of the Lasserre hierarchy), that is solved using *Hamiltonian Updates (HU)* [GBKSF22, HTO⁺25], providing a classical and a quantum version of the algorithm.
- (3) solving the QUBO directly without an intermediate relaxation via classical, specialized QUBO solvers, e.g. [RKS23, CJMM22], or *quantum annealing* [Sys].

All of these methods have been implemented and there exist various experimental evaluations of these methods. In this article, we focus in particular (but not exclusively) on a comparison of the methods listed in the first two points, i.e. the SOS based methods, referred to as *SOS-SDP*, and HU.

In this interdisciplinary study we provide a vast experimental comparison of a broad range of methods and solvers for solving SDP relaxations of QUBOs formulations of two common problems in logistics. We choose these sets of problems, as applications in science and engineering regularly lead to highly non-generic optimization problems, which are known to behave differently than randomly generated data. Specifically, we investigate the *(open) vehicle routing problem (OVRP)* concerning the distribution of goods carried out with a fleet of transporters, and the *(affinity-based) slotting problem (ASP)* concerning the optimal storage of goods in warehouses. The problems in our study are represented by *real-world data* – in opposition to using generated, random instances – which is provided by the industry partner 4flow SE. We chose the OVRP and ASP instances not only because they can be reformulated as QUBOs, their practical relevance, and the availability of real-world data, but also because they are natural candidates for benchmarking: The original mathematical representation of the problems are *integer programs (IP)* and *integer quadratic programs (IQP)*, respectively, so that IP/IQP solvers can still effectively solve the specific instances and thus provide benchmarks. This allows us to not only compare the different approaches among each other, but also make qualitative statements about their effective quality on these problem sets.

In terms of the SDP methods, we focus in particular on different software and solvers for SOS-SDP based hierarchies, and on HU. We highlight that we do not intend to propose a specific approach, but give a qualitative comparison and highlight abilities and challenges for the different methods. All results, logs, and a full documentation of the experiments are available via

https://moto.math.nat.tu-bs.de/appliedalgebra_public/sdp_qubo_benchmarking.

Results. Our main results are:

- (1) Due to the IP/IQP structure of the original problem instances, our approach requires a two-step reformulation: First, we reformulate the instances as a QUBO, which we then relax as an SDP, see Figure 1. Hence, we expected that the chosen problems are

challenging for all chosen methods. The experiments confirm this expectation, showing that all methods and solvers that are not directly working on the IP/IQP side have significant problems with solving the corresponding SDPs; see Subsection 6.3 and in particular Table 6 and Figure 8.

- (2) Despite the general challenges, we see significant differences in terms of quality of bounds and running times of the different methods. In particular, we see that
 - on the SDP-SOS side there is a broad range of qualitative differences. In several cases, we observed that the SDP solvers had both memory and numerical problems. In terms of quality of the results, the software TSSOS [WML19], which exploits sparsity, joint with the MOSEK [ApS24] SDP solver obtained the best results.
 - HU does not outperform the best SOS-SDP results in terms of quality. However, the running time of HU is mainly based on the chosen precision, which allows both to tackle larger size problems, and to compute very rough bounds quickly. Moreover, in contrast to SOS-SDP, it always provides solution recovery.
- (3) Recently, SDP solvers as well as software for preprocessing were developed that specifically exploit the problem’s properties, e.g. sparsity, low rank or matrix structures. In summary, we confirm the potential for improvement given by the application of such specialized software. Additionally, we see that methods can perform differently or worse on real-world data, showing the importance of including non-randomly generated instances in software developments and benchmark studies.
- (4) This finding is mirrored on the quantum side. Quantum algorithms research is facing the issue that benchmarks are difficult to perform, due to the absence of larger-scale quantum hardware. By necessity then, results on the performance of quantum algorithms typically rely on strong assumptions and often pertain only to asymptotic behavior of generic approaches. What we see here is that the assessment of quantum-algorithmic performance for real-world problems is not adequately captured by these high-level arguments. Practitioners who want to gauge the impact of quantum computing for their use cases will find that the running time of quantum solutions for their specific instances may fall widely short of promises based on asymptotics.

Organization. This article is organized as follows: After brief preliminaries in Section 2, we introduce background on our two problem classes, OVRP and ASP, in Subsection 3.1 and Subsection 3.2, respectively, and explain their reformulation from IP/IQP to QUBO structure in Subsection 3.3. In Section 4 we provide background on the SOS-SDP relaxation, and in Section 5 on the Hamiltonian Updates algorithm both from a classical and a quantum perspective. In the main Section 6 we present the experimental results: We recall the experimental setup in Subsection 6.1, provide benchmarks from IP/IQP and QUBO formulation in Subsection 6.2, and the results from the SDP relaxations in Subsection 6.3, followed by a discussion in Subsection 6.4. We conclude the paper in Section 7. Several further technical details are specified in Appendices A to E.

Related Work. There exists a large range of articles related to this study. First, regarding the SOS-SDP relaxation there are various general introductions e.g. [Lau09, Las15, The24], and in particular several works on using Lasserre’s hierarchy on binary optimization problems and their convergence guarantees [Lau03, FSP16, STKI17].

In the context of CPOPs and QUBOs various colleagues made significant effort in providing experimental studies and comparisons. There exists a collection of benchmark problem sets and corresponding studies, e.g. [Wie07, FTB⁺18, Mit24].

Related to combinatorial optimization problems discussed here, there are works benchmarking MaxCut algorithms, including the approximation algorithm by Goemans and Williamson, on instances, among other, from real-world graphs from the network library [MW23]. Moreover, SDP relaxations were applied to various other applications resulting in benchmarking articles. A famous recent example is the application of sparsity variants of the SOS based hierarchies to the Alternating-Current Optimal Power Flow Problem using different solvers, e.g. TSSOS [MW21, GH22], and SPARSEPOP [GMM16]. Another example is the overview [AM16] displaying SOS-SDP (and SDSOS) relaxations for polynomial optimization problems from Operations Research and Transportation Engineering.

In this article we use a wide range of solvers for our experiments. There are several works benchmarking these solvers on random instances: [HKS23] developed the LORAINE solver and tested it on randomly generated MaxCut and QUBO instances with $n = 50$ variables, comparing it to the standard, commercial SDP solver MOSEK [AA00, ApS24]. Similarly, MANISDP [WH24] solved second order Lasserre relaxations on randomly generated QUBOs with up to $n = 120$ variables, likewise comparing the results to MOSEK. The solver COSMO [GCG21] is benchmarked on several randomly generated SDP instances.

Hamiltonian Updates was developed in [GBKSF22]. It was improved and benchmarked on randomly generated instances in [HTO⁺25]. The quantum running time analysis uses a similar gate count approach as [AHR⁺23, DCS⁺23, BMN⁺21, CKM19].

Furthermore, beyond SDP based methods, [JLM⁺21] tested QUBO problems with D-Wave’s quantum annealing procedure against branch-and-bound and SDP methods, reporting better results than the classical methods on these particular methods, and [HXL⁺23] compared quantum annealing and quantum inspired annealers on quadratic assignment problems.

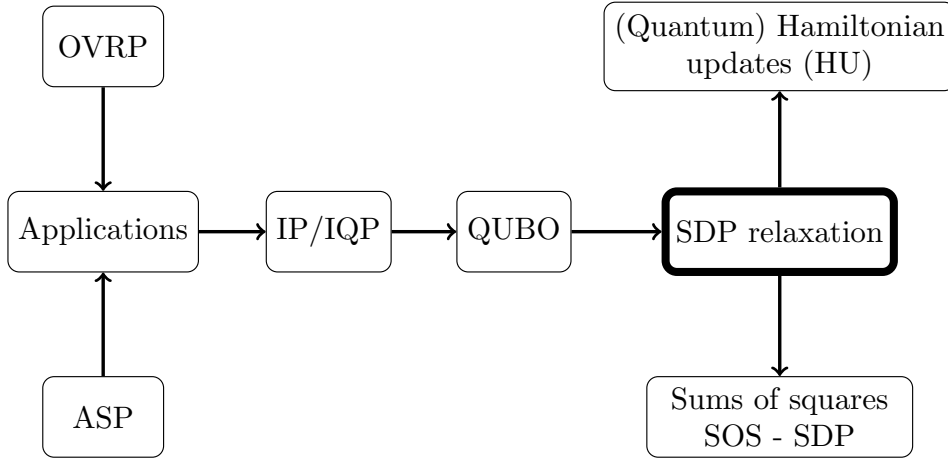


FIGURE 1. Visualization of the pipeline for this work: We compare different methods and software for semidefinite programming (SDP) relaxations of quadratic unconstrained binary optimization (QUBO) formulations that emerge from real-life applications. In particular, we consider the open vehicle routing problem (OVRP) and the affinity-based slotting problem (ASP). The applications are initially formulated as integer program (IP) or integer quadratic program (IQP) with either a linear objective function (for OVRP) or a quadratic objective function (for ASP), respectively, that can be solved to optimality.

2. PRELIMINARIES

We give an overview on the basic notation and definitions that are essential in the upcoming sections. The method specific definitions each appear in the beginning of the respective Sections 3 to 5. We refer to the set of *natural*, *integer* and *real* numbers by \mathbb{N} , \mathbb{Z} and \mathbb{R} respectively, and thus denote $\mathbb{Z}_{\geq 0} = \{x \in \mathbb{Z} \mid x \geq 0\}$ and $\mathbb{R}_{\geq 0} = \{x \in \mathbb{R} \mid x \geq 0\}$. We use bold letters to denote vectors, e.g. $\mathbf{x} = [x_1 \dots x_n]^T \in \mathbb{R}^n$. With the letter T we indicate the transpose of a vector or matrix. In this article, we specifically consider *real symmetric* matrices $A = (a_{ij})_{1 \leq i, j \leq n} \in \mathbb{R}^{n \times n}$ with $A^T = A$. A symmetric matrix $A \in \mathbb{R}^{n \times n}$ is *positive semidefinite* if and only if $\mathbf{x}^T A \mathbf{x} \geq 0$ for all $\mathbf{x} \in \mathbb{R}^n$, and we indicate this via the notation $A \succcurlyeq 0$. For two matrices $A, B \in \mathbb{R}^{n \times n}$ we define their *inner product* $\langle A, B \rangle = \text{trace}(A^T B) = \sum_{i,j} a_{ij} b_{ij}$.

Let $r \in \mathbb{N}$ and $C, A_1, \dots, A_r \in \mathbb{R}^{n \times n}$ be symmetric matrices and $\mathbf{b} \in \mathbb{R}^r$. A *semidefinite optimization problem (SDP)* is of the following form

$$\begin{aligned} \min_{X \in \mathbb{R}^{n \times n}} \quad & \langle C, X \rangle \\ \text{subject to} \quad & \langle A_i, X \rangle = b_i \text{ for all } i = 1, \dots, r \\ & X \text{ symmetric, } X \succcurlyeq 0. \end{aligned}$$

In this article, we consider SDPs that emerge as relaxations of *quadratic unconstrained binary optimization problems (QUBOs)*. Let $Q \in \mathbb{R}^{n \times n}$ be a symmetric matrix. Then a QUBO is of the form

$$(2.1) \quad \min_{\mathbf{x} \in \{0,1\}^n} \mathbf{x}^T Q \mathbf{x}$$

In (2.1), we define the QUBO via optimizing over the set $\{0, 1\}^n$. Alternatively, one can define a QUBO over $\{1, -1\}^n$. This formulation is often called *Ising model* in the physics context and we use it mostly in Section 5. We give the conversion between both formulations in Appendix C.

3. INDUSTRY PROBLEMS AND QUBO REFORMULATIONS

In this section, we introduce two business-relevant combinatorial optimization problems. Our industry partner, 4flow SE, provided data stemming from their work with customers on real-world problems. In what follows, we refer to this data by *real-world data*. In particular, we consider a *vehicle routing problem (VRP)* and an *affinity-based slotting problem (ASP)*.

3.1. Vehicle Routing Problems. The *vehicle routing problem (VRP)* is an extension of the well-studied and NP-hard *traveling salesman problem (TSP)*. State-of-the-art heuristics, such as [Hel00], and exact solvers like Concorde [ABCC] can effectively solve TSP instances involving thousands of nodes. However, these approaches are highly specialized for the TSP and are generally not applicable in industrial settings. Generic TSPs rarely occur in practice, since most problems come with additional constraints such as vehicle capacities and complex operating costs that are not only limited to distance.

The VRP was first formally introduced in [DR59] and involves minimizing the total distance traveled by a fleet of vehicles serving a set of customers. For a basic overview of the numerous VRP variants, we refer the reader to [TV02]. Solutions to industrial-sized VRPs are generally limited to heuristics built upon TSPs such as [Hel17] or more robust methods such as taboo searches like [TGGP01] and large neighborhood searches like [RP06]. Our work is concerned with a common variant of the VRP called the *open vehicle routing problem (OVRP)* where vehicles are not forced to return to the depot after serving all the customers [YJR16]. The

OVRP is very common in inbound logistics of the automotive industry, for example. We define a specific type of OVRP that we consider throughout this article. It is an *integer program (IP)*.

3.1.1. Open Vehicle Routing Problem with Stop Constraints and a Fixed Fleet. The *OVRP with stop constraints and a fixed number of vehicles* is a variant of the IP introduced in [YJR16] like that in [Bor17] with the well-known extension of the *subtour elimination constraints* of Miller-Tucker-Zemlin (MTZ) for the TSP [MTZ60].

In Tables 1 and 2, we give an overview of the variables used in the OVRP formulation.

Index	Sets	Description
i, j	V	Generic set of all nodes including depot
0	–	Depot node
k	K	Set of available vehicles
n	$V \setminus \{0\}$	Number of customer nodes

TABLE 1. Definitions for the indices and labels appearing in the IP in (3.2)-(3.9).

Name	Domains	Description
d_{ij}	$\mathbb{R}_{\geq 0}$	Distance between nodes i and j
C_k^{fixed}	$\mathbb{R}_{\geq 0}$	Fixed cost of each vehicle k
$C_k^{\text{per dist}}$	$\mathbb{R}_{\geq 0}$	Cost per distance for vehicle k
$C_k^{\text{per stop}}$	$\mathbb{R}_{\geq 0}$	Cost for a vehicle k to stop at a node in $V \setminus \{0\}$
maxstop_k	$\mathbb{Z}_{\geq 0}$	Max number of stops allowed in $V \setminus \{0\}$ for each k
x_{ijk}	$\{0, 1\}$	Decision variable for if k connects i to j
u_i	$\mathbb{Z}_{\geq 0}$	The order in which node i is visited
Z_{OVRP}	$\mathbb{R}_{\geq 0}$	The objective value, viz. the total cost incurred

TABLE 2. Definitions for the cost factors, constraint bounds, and variables appearing in the IP in (3.2)-(3.9).

Let

$$(3.1) \quad Z_{\text{OVRP}} = \sum_{k \in K} \sum_{i, j \in V} C_k^{\text{per dist}} d_{ij} x_{ijk} + \sum_{k \in K} \sum_{\substack{i, j \in V \\ j \neq 0}} C_k^{\text{per stop}} x_{ijk} + \sum_{k \in K} \sum_{j \in V \setminus \{0\}} C_k^{\text{fixed}} x_{0jk}.$$

Then the IP for the OVRP with stop constraints can be formulated as

$$(3.2) \quad \min \quad Z_{OVRP}$$

$$(3.3) \quad \text{subject to} \quad \sum_{\substack{i \in V \\ k \in K \\ i \neq j}} x_{ijk} = 1, \quad \text{for all } j \in V \setminus \{0\},$$

$$(3.4) \quad \sum_{\substack{j \in V \setminus \{0\} \\ k \in K \\ i \neq j}} x_{ijk} \leq 1, \quad \text{for all } i \in V \setminus \{0\},$$

$$(3.5) \quad \sum_{\substack{i \in V \\ i \neq j}} x_{ijk} - \sum_{\substack{i \in V \setminus \{0\} \\ i \neq j}} x_{jik} \geq 0, \quad \text{for all } k \in K, \text{ for all } j \in V \setminus \{0\},$$

$$(3.6) \quad u_i - u_j + 1 \leq n(1 - \sum_{k \in K} x_{ijk}), \quad \text{for all } i, j \in V \setminus \{0\} \text{ with } i \neq j,$$

$$(3.7) \quad \sum_{\substack{i \in V \\ j \in V \setminus \{0\} \\ i \neq j}} x_{ijk} \leq \text{maxstop}_k, \quad \text{for all } k \in K,$$

$$(3.8) \quad 1 \leq u_j \leq n, \quad \text{for all } j \in V \setminus \{0\},$$

$$(3.9) \quad x_{ijk} \in \{0, 1\}, \quad \text{for all } i, j \in V, \text{ for all } k \in K.$$

Constraint (3.3) guarantees that every customer node is entered exactly once. Constraint (3.4) guarantees that each customer is left *at most* once. Constraint (3.5) is a type of flow constraint making sure that customer nodes cannot act as sources. Constraint (3.6) is the MTZ-Subtour elimination constraint, forcing vehicles to have a tour connected with the depot. Constraint (3.7) restricts the number of stops each vehicle can make. Constraints (3.8) and (3.9) define the domains for each of the variables.

3.1.2. The Instances. In what follows, we describe two small real-world instances for OVRP. We point out that our OVRP instances are small by industry standards. As a comparison, most OVRPs range from 50-200 customers.

Data Preparation. The original real-world data includes geographic coordinates and other sensitive information that we anonymize: We replace the coordinates with a distance matrix using the great circle distance as well as remove names of locations, references to company names, vehicle makes and models.

Assumptions and Key Features. We briefly enumerate the underlying assumptions and key features of the two instances:

- We label the instances by OVRP15 and OVRP11, with 14 and 10 customer nodes, respectively. Each instance has a single depot node. Note that this leads to 15 and 11 total nodes, respectively.
- The instances are OVRPs with a homogeneous fleet of vehicles. This means that C_k^{fixed} , $C_k^{\text{per dist}}$, and $C_k^{\text{per stop}}$ in Table 2 are all independent of k .
- There are no capacity constraints, since the total demand in the original customer problem did not exceed a single vehicle capacity.
- Each vehicle cannot make more than three stops, i.e., $\text{maxstop}_k = 3$ for all k in (3.7).

- We assume that each instance uses the minimum number of vehicles needed to solve the problem, which comes from the maxstop constraint in Equation (3.7):

$$\begin{aligned} \text{minimum number of vehicles for OVRP15} &= \left\lceil \frac{14}{3} \right\rceil = 5, \\ \text{minimum number of vehicles for OVRP11} &= \left\lceil \frac{10}{3} \right\rceil = 4. \end{aligned}$$

We constrain the number of vehicles to the smallest possible number in order to keep the QUBOs as small as possible. Notice that under this assumption, the fixed costs in Equation (3.1) no longer play a role.

3.2. Slotting Problems. The field of logistics offers a variety of non-linear optimization problems. Of particular interest for this work are problems that are inherently quadratic optimization problems. For example, optimally storing and retrieving items within warehouses is related to quadratic assignment problems [Çel99] and routing problems, such as the TSP. We introduce a type of slotting problem, which is an *integer quadratic program (IQP)*.

3.2.1. Affinity-based Slotting. We note that the IQP discussed in this section is essentially a special case of a *generalized quadratic assignment problem (GQAP)* [LM04]. Many works have studied GQAPs in the context of warehouses where instead of flow matrices, affinity matrices are used in the objective function [LMMT⁺21, CLL12, WJW21, LCY20, LMN16, HXL⁺23]. Warehouses aim to ease the storing and procurement of goods for a company. Each warehouse stores an amount of products or materials of different *material types* \mathcal{M} available for purchase or further shipment. Based on order history, one can determine which material types are generally ordered together and thus also need to be retrieved or “picked” together. This is the concept of *pairwise affinity*. We represent pairwise affinity for a pair of material types $m, n \in \mathcal{M}$ by an element of an *affinity matrix* $\sigma \in \mathbb{R}_{\geq 0}^{|\mathcal{M}| \times |\mathcal{M}|}$. An element of σ is generally larger for materials that are often ordered together, and smaller otherwise. There are numerous ways to define σ in the literature such as the *Jaccard Measure* [Jac01] and the *Bindi Measure* [BMPR09], see [Kof15] for an overview.

Given σ and a set of material types \mathcal{M} , assume that we have access to a sequence of orders, and a set of storage locations that are partitioned into aisles A_1, \dots, A_k . Each aisle, for $j = 1, \dots, k$, has a *capacity* $|A_j|$, which corresponds to the amount of material types that can fit in a single aisle. The goal is to assign each material type $m \in \mathcal{M}$ to an aisle A_j such that we minimize the *cost* of retrieving all orders.

In this work, we consider the *affinity-based slotting problem (ASP)*, where the cost function aims to minimize the number of *aisle changes* in order to find the minimal travel distance for retrieving all materials. This problem can be shown to be NP-hard, for example, by reducing the problem to a perfectly balanced bipartition problem [Now24, GJS74]. To model the ASP, let $x_{mj} \in \{0, 1\}$ be equal to 1 if material type m is assigned to aisle A_j , and 0 otherwise. If different material types $m \neq n$ are placed in different aisles A_i and A_j with $A_i \neq A_j$, we impose

a price proportional to their affinity σ_{mn} . We formulate the ASP as an IQP in (3.10).

$$(3.10) \quad \min Z_{ASP} = \min \sum_{m,n \in \mathcal{M}} \sum_{\substack{i,j=1 \\ i \neq j}}^k \sigma_{mn} x_{mi} x_{nj}$$

$$(3.11) \quad \text{subject to} \quad \sum_{j=1}^k x_{mj} = 1 \quad \text{for all } m \in \mathcal{M}$$

$$(3.12) \quad \sum_{m \in \mathcal{M}} x_{mj} \leq |A_j| \quad \text{for all } j = 1, \dots, k$$

$$(3.13) \quad x_{mj} \in \{0, 1\} \quad \text{for all } m \in \mathcal{M}, j = 1, \dots, k.$$

The constraint (3.11) forces each material to be assigned to exactly one aisle. Constraint (3.12) ensures that the capacity of each aisle is not exceeded. The final constraint in (3.13) defines the domain for the problem variables. For more details, see Appendix A.1.

3.2.2. The Instances. Given the ASP formulation in (3.10), we provide three data sets using an affinity matrix σ derived from real-world data.

Data Preparation. These instances are *based* on real order data. The order data comes from a warehouse containing over 4000 orders over a year-long period. The 30, 60, 90 most popular material types across all orders were determined, and then the affinity matrices σ were constructed using the Jaccard measure [Jac01].

Assumptions and Key Features. We briefly describe the underlying assumptions and key features of the instances. We provide three instances that we label by ASP30, ASP60, ASP90, where the corresponding number denotes the number of material types. Each dataset has three aisles A_j for $j = 1, 2, 3$ with equal capacities $|A_1| = |A_2| = |A_3|$. The sum of the three aisle capacities equals the total number of materials. For example, ASP30 is a dataset with a total capacity of 30 material types and aisle capacities of ten storage locations. Note that, we limit the number of aisles to $k = 3$ in order to keep the problem sizes small enough to provide an optimal solution via a standard quadratic solver that we can compare with the SDP relaxations via SOS-SDP and HU. However, limiting $k = 3$ is an extreme underestimate of the real-world situation. Customers regularly have warehouses with $k > 10$.

3.3. Reformulation as QUBO. After formally defining the problems as IP and IQP models, we transform the formulation into a quadratic unconstrained binary optimization (QUBO) problem, see Equation (2.1), which we further relax in the upcoming sections. For the conversion from IP to QUBO, we follow the methodology developed by Glover et al. [GK18]. The same approach can be applied to convert an IQP to QUBO, as the constraints are linear and the objective function is quadratic.

Essentially, converting an IP/IQP model into a QUBO problem involves three steps:

- (1) **Unconstraining**, which involves transforming constraints into terms that can be incorporated into the objective function.
- (2) **Binarization** is applied where integer variables are redefined as binary, ensuring the optimization problem fits within the binary framework of QUBO.
- (3) **Penalization** to ensure that any violation of the original constraints is appropriately penalized.

In Appendices A.2.1 to A.2.3 we show the conversion of the IQP formulation to its QUBO formulation in detail, using ASP30 as an example.

The modeling and conversion process is carried out using *GAMS* (*General Algebraic Modeling System*), a platform for formulating and solving large-scale mathematical optimization problems. GAMS provides the flexibility to implement the transition from IP/IQP to QUBO efficiently and the computational power necessary to solve both types of problems. In particular, the GAMS reformulation tool QUBO_SOLVE, see Subsection 6.1, is employed to transform the original IP/IQP models in the GAMS language into the QUBO formulation (2.1), facilitating the solving of the QUBO problem as described in the later sections. This tool also supports solving the problem using either classical solvers such as e.g. CPLEX [Cpl09] and GUROBI [Gur24] or hybrid quantum methods such as D-Wave’s quantum annealing procedure [Sys]. It is important to note that the objective value obtained after solving the QUBO to optimality will be equal to the optimal value of the original IP/IQP formulation, as both the models are equivalent, see [GH20] and [CJY⁺22].

4. SOS-SDP RELAXATION

In this section we interpret QUBOs as a *polynomial optimization problem on the boolean hypercube*. We recall that in the QUBO formulation (2.1) we are given a symmetric matrix $Q = (q_{ij})_{1 \leq i, j \leq n} \in \mathbb{R}^{n \times n}$, and our goal is to minimize $\mathbf{x}^T Q \mathbf{x}$ with $\mathbf{x} \in \{0, 1\}^n$. Rewriting this problem as a polynomial optimization problem, we aim to apply a *sums of squares (SOS) hierarchy relaxation* that leads to solving a semidefinite program (SDP). In Subsection 4.1 we give an overview on the interpretation as polynomial optimization problem and in Subsection 4.2 we motivate how to derive the SDP relaxation from the SOS approach. We explain the software that we use for the SOS relaxation in Subsection 4.3.

4.1. The QUBO as Polynomial Optimization Problem. Let $\mathbb{R}[\mathbf{x}] = \mathbb{R}[x_1 \dots x_n]$ be the polynomial ring of *real n -variate polynomials*. Rewriting the target function from the given QUBO as in Equation (2.1) we can consider the following polynomial $p(\mathbf{x}) \in \mathbb{R}[\mathbf{x}]$ with n variables of degree two:

$$\begin{aligned}
 p(\mathbf{x}) &= \mathbf{x}^T Q \mathbf{x} \\
 (4.1) \quad &= [x_1 \quad x_2 \quad \dots \quad x_n] \begin{bmatrix} q_{11} & q_{12} & \dots & q_{1n} \\ q_{12} & q_{22} & \dots & q_{2n} \\ \vdots & \vdots & \ddots & \vdots \\ q_{1n} & q_{2n} & \dots & q_{nn} \end{bmatrix} \begin{bmatrix} x_1 \\ x_2 \\ \vdots \\ x_n \end{bmatrix} \\
 &= q_{11}x_1^2 + 2q_{12}x_1x_2 + \dots + 2q_{1n}x_1x_n + q_{22}x_2^2 + \dots + 2q_{2n}x_2x_n + \dots + q_{nn}x_n^2.
 \end{aligned}$$

Furthermore, we rewrite the binary constraints $\mathbf{x} \in \{0, 1\}^n$ as polynomial equality constraints:

$$(4.2) \quad x_i(x_i - 1) = 0 \text{ for all } 1 \leq i \leq n.$$

Using the polynomial target function from (4.1) and the polynomial constraints (4.2) we obtain a *constrained polynomial optimization problem (CPOP)* as interpretation of the given QUBO. Equivalently to minimizing $p(\mathbf{x})$, we can formulate this as a problem of *nonnegativity*:

$$(4.3) \quad \begin{aligned} &\max && \lambda \in \mathbb{R} \\ &\text{subject to} && p(\mathbf{x}) - \lambda \geq 0 \text{ for all } \mathbf{x} \in \{0, 1\}^n. \end{aligned}$$

Polynomial optimization problems are NP-hard in general. However, the idea of the nonnegativity formulation in (4.3) offers the use of relaxations in terms of *certificates of nonnegativity*. These are sufficient conditions showing a polynomial $f(\mathbf{x})$ is nonnegative, i.e., in the

unconstrained case $f(\mathbf{x}) \geq 0$ for $\mathbf{x} \in \mathbb{R}^n$, and the conditions are effectively computable. A widely used certificate of nonnegativity is to show that a polynomial $f(\mathbf{x})$ can be written as $f(\mathbf{x}) = \sum_{i=1}^{\ell} s_i(\mathbf{x})^2 \in \mathbb{R}[\mathbf{x}]$, i.e., $f(\mathbf{x})$ is a sum of squared polynomials $s_i(\mathbf{x})$. We refer to this relaxation as *sum of squares (SOS)* relaxation and to a polynomial that can be written as such decomposition likewise as *SOS* (polynomial). For an overview on polynomial optimization and SOS see e.g. [Lau09, Las15, The24] and Appendix B for an overview on other certificates of nonnegativity beyond SOS.

4.2. Deriving the SDP relaxation. We aim to apply an SOS relaxation on (4.3) which leads to solving an SDP. For an intuition, we first consider unconstrained polynomial optimization.

Gram Matrix Method. Let $f(\mathbf{x})$ be a polynomial in n variables and of degree $2d$. We want to determine whether f is SOS. Let \mathbf{m}_d be the vector that contains all monomials (e.g. $1, x_1, x_2, x_1^2, x_1x_2, \dots$) with n variables up to degree d . A symmetric matrix G is positive semidefinite if and only if there exists a *Cholesky decomposition*, i.e., there exists a matrix B with $B^T B = G$.

We aim to find a *Gram matrix* $G \in \mathbb{R}^{\binom{n+d}{d} \times \binom{n+d}{d}}$ containing the corresponding coefficients of $f(\mathbf{x})$ such that $\mathbf{m}_d^T G \mathbf{m}_d = f(\mathbf{x})$. If and only if G is positive semidefinite and thus permits the Cholesky decomposition $G = B^T B$, then

$$f(\mathbf{x}) = \mathbf{m}_d^T G \mathbf{m}_d = \mathbf{m}_d^T B^T B \mathbf{m}_d = (B \mathbf{m}_d)^T B \mathbf{m}_d = \sum s_i(\mathbf{x})^2,$$

i.e., we can write $f(\mathbf{x})$ as a sum of squared polynomials $s_i(\mathbf{x})$.

Unconstrained Polynomial Optimization. The Gram-Matrix-Method can be combined with semidefinite programming [Par00]: Using the definition of \mathbf{m}_d as above, the unconstrained problem of nonnegativity $\max_{\lambda \in \mathbb{R}} \{p(\mathbf{x}) - \lambda \geq 0 \text{ for all } \mathbf{x} \in \mathbb{R}^n\}$ turns into the SDP relaxation:

$$\begin{aligned} \max \quad & \lambda \in \mathbb{R} \\ \text{subject to} \quad & p(\mathbf{x}) - \lambda = \mathbf{m}_d^T G \mathbf{m}_d \\ & G \succcurlyeq 0. \end{aligned}$$

We optimize over the entries of a Gram matrix G with linear constraints that refer to the coefficients of the polynomial $p(\mathbf{x}) - \lambda$ with the requirement that G is positive semidefinite. Thus, we have to solve an SDP.

Constrained Polynomial Optimization. After this intuition in the unconstrained case we again consider our original CPOP in (4.3) which we derived from the given QUBO. Putinar's [Put93] Positivstellensatz uses the idea to express a polynomial in terms of polynomial constraints $h_i(\mathbf{x}) = 0$, for $i = 1, \dots, n$ and SOS polynomials $s_i(\mathbf{x})$ for $i = 0, \dots, n$ to certify nonnegativity. This leads to a method known as *Lasserre's hierarchy* [Las01] that tackles the problem:

$$(4.4) \quad \begin{aligned} \max \quad & \lambda \in \mathbb{R} \\ \text{subject to} \quad & p(\mathbf{x}) - \lambda = s_0(\mathbf{x}) + \sum_{i=1}^n s_i(\mathbf{x}) h_i(\mathbf{x}) \\ & \text{degree}(s_0(\mathbf{x})) \leq 2d \text{ and } \text{degree}(s_i(\mathbf{x}) h_i(\mathbf{x})) \leq 2d \quad \text{for all } 1 \leq i \leq n \\ & s_0(\mathbf{x}) \text{ is SOS and } s_i(\mathbf{x}) \text{ are SOS} \quad \text{for all } 1 \leq i \leq n \end{aligned}$$

Problem (4.4) again results in solving an SDP: We aim to find polynomials $s_i(\mathbf{x})$ that are SOS. The polynomials $s_i(\mathbf{x})$ are unknown and we optimize over their corresponding Gram matrices, restricting their degree. By increasing the allowed degree $2d$ we compute a sequence of SDP relaxations. This sequence leads to *sequence of lower bounds* that – under mild assumptions, are

fulfilled in the QUBO case – eventually converges to the actual optimum of (4.3) [FSP16, Las01]. In fact, the approach by Lasserre [Las01] uses the theory of *moments* and is dual to (4.4). For further details, see [Las15, The24].

Note that, the involved Gram matrices in the sequences of lower bounds grow very large in practice. They have a size of $\binom{n+2d}{2d} \times \binom{n+2d}{2d}$ for a polynomial with n variables and degree $2d$. The size increases exponentially, as we increase the degree in the hierarchy. For our problems, the number of variables n ranges between $96 \leq n \leq 3380$ and we see that for our problems, even the first order Lasserre relaxation with $2d = 2$ is challenging for SDP solvers, see Section 6.

4.3. Solving the SOS relaxation. In order to compute the SOS-SDP relaxation as described before we work with academic software used in polynomial optimization to derive the SDP relaxations of the QUBOs. Then an SDP solver is called internally to solve those SDPs. We give an overview on the tested software below. In preliminary experiments, we additionally tested the software GLOPTIPOLY [HL03] on MATLAB. We did not pursue this further since the software struggled with large input matrices.

SumOfSquares.jl The JULIA package [SUMOFSQUARES.JL \(SOS.JL\)](#) [LCD⁺17, WLC⁺19] performs unconstrained and constrained SOS optimization as described above. We input the given QUBO matrix and convert it to a polynomial representation. The SOS.JL package allows to input the relaxation order as in (4.4) automatically derives the corresponding SDP. Then, internally, the package calls an SDP solver to solve the resulting SDP. We test the internal SDP solvers [MOSEK](#) [ApS24] and [LORAINE](#) [HKS24].

TSSOS The JULIA software [TSSOS](#) [WML19][MW21] by Wang, Magron and Lasserre improves the above described moment SOS hierarchy along with tools to exploit sparsity in the given polynomial [WML20b][WML20a] (“TS” stands for “term sparsity”) by exploring block structures in the matrices. Similar to SOS.JL, TSSOS uses the polynomial representation and then automatically derives the corresponding SDPs. As SDP solver, internally, TSSOS provides an interface for MOSEK and [COSMO](#) [GCG21]. Especially, the extension CS-TSSOS [WMLM21] (“CS” stands for “chordal sparsity”) is suitable for large-scale polynomial optimization problems. Earlier works on chordal sparsity include the software [SPARSEPOP](#) [WKK⁺08], that we do not test here.

SDP solvers Inside of SOS.JL and TSSOS, we call the following SDP solvers as described above: The SDP solver MOSEK is a state-of-the-art but general purpose interior-point method SDP solver. As shown in Section 6, while we achieve the best results on our instances with MOSEK inside TSSOS, we experience that the large-scale SDPs cannot be solved. Additionally, we use the low-rank interior-point SDP solver LORAINE for JULIA. It has been reported that often with LORAINE the second order relaxation already converges to the optimal solution, outperforming MOSEK on randomly generated MaxCut and QUBO instances [HKS23]. The solver COSMO does not perform interior-point methods but is based on the alternate direction of multipliers method (ADMM) and is suitable for large-scale convex optimization problems.

Next to the polynomial optimization software TSSOS and SOS.JL, we also solve the SOS-SDP relaxation directly via available academic SDP solvers: The MATLAB solver [MANISDP](#) [WH24] based on MANOPT [BMAS14] is tailored for low-rank SDPs and uses manifold optimization. It has been used to solve the second order Lasserre relaxation ($2d = 4$) on QUBOs up to $n = 120$ variables, outperforming MOSEK. [WH24]. For this solver, we use the Ising formulation, see Appendix C, as input. Likewise, we use the [SPLITTING CONIC SOLVER\(SCS\)](#) [OCPB23] with its default settings, as a standard an open source convex cone solver, directly on this formulation.

5. HAMILTONIAN UPDATES: CLASSICAL AND QUANTUM

In this section, we give an overview on the SDP relaxation via the *Hamiltonian Updates algorithm (HU)*, developed in [GBKSF22] and improved by [HTO⁺25]. The advantage of HU is its favorable scaling in the problem size compared to standard SDP solvers at the cost of a rather expensive polynomial dependence in the precision. This makes HU more suitable to applications where high precision is less important: This is for example the case when we use the solution of the SDP as input to a randomized rounding procedure, which is approximate by its nature. Additionally, through the randomized rounding procedure, HU provides lower and upper bounds for the optimal value, as well as a feasible solution for the original problem.

5.1. Problem formulation. For HU, we consider a slightly reformulated QUBO problem of the form

$$(5.1) \quad \begin{aligned} \max_{\mathbf{x} \in \mathbb{R}^n} \quad & \sum_{i,j=1}^n C_{ij} x_i x_j \\ \text{subject to} \quad & x_i = \pm 1, \end{aligned}$$

which we call an *Ising model* with a cost matrix $C \in \mathbb{R}^{n \times n}$. As shown in Appendix C, one can easily convert a problem given in QUBO form (2.1) into the Ising formulation (5.1). We can then relax (5.1) into the following SDP:

$$(5.2) \quad \begin{aligned} \max_{X \in \mathbb{R}^{n \times n}} \quad & \langle C, X \rangle \\ \text{subject to} \quad & \text{diag}(X) = 1 \\ & X \succeq 0. \end{aligned}$$

Goemans and Williamson [GW95] developed a *randomized rounding* procedure that, given a solution for the SDP relaxation (5.2), outputs a feasible solution for the original Ising problem. In addition, for cost matrices of specific forms, this method comes with rigorous approximation guarantees, e.g. applied to the original MaxCut formulation with nonnegative edge weights, the randomized rounding procedure by Goemans and Williamson gives the famous result of an expected value that is at least 0.87856 times as large as the optimal value [GW95].

For the randomized rounding, we first factorize the optimizer $X^* \in \mathbb{R}^{n \times n}$ of the SDP in (5.2) as $X^* = B^T B$ with a symmetric matrix $B \in \mathbb{R}^{n \times n}$. Then the sign of the column-wise projection of B onto a Gaussian random vector $\mathbf{g}_i \in \mathbb{R}^n$ gives the entries of a vector $\mathbf{x} \in \{\pm 1\}^n$ that is an approximate solution to (5.1). We summarize this rounding procedure as

$$(5.3) \quad \begin{aligned} \text{compute} \quad & B = \sqrt{X^*}, \\ \text{sample} \quad & \mathbf{g}_i \stackrel{\text{iid.}}{\sim} \mathcal{N}(0, 1), \quad i = 1, \dots, n \\ \text{compute} \quad & x_j \leftarrow \text{sign} \left(\sum_i \mathbf{g}_i B_{ij} \right), \quad j = 1, \dots, n. \end{aligned}$$

where $\sqrt{X^*} \in \mathbb{R}^{n \times n}$ denotes a symmetric matrix with $\sqrt{X^*}^T \sqrt{X^*} = X^*$ and $\mathcal{N}(0, 1)$ is a normal distribution with a mean 0 and variance 1.

5.2. Solving the SDP using Hamiltonian Updates. The idea behind HU is to express X as a *Gibbs state*, an object known from quantum mechanics. The physical context of this is not further relevant here since the HU routine itself is purely classical. Nevertheless, this inspiration

from quantum mechanics is a natural choice for positive semidefinite matrices, and gives rise to a possible quantum speedup [vAG19]. The Gibbs state is given by

$$(5.4) \quad \rho_H = \frac{\exp(-H)}{\text{tr}(\exp(-H))} \in \mathbb{R}^{n \times n}$$

for some symmetric $H \in \mathbb{R}^{n \times n}$, called the *Hamiltonian*, and we set $X = n\rho_H$. This construction makes X manifestly positive semidefinite. Then, by introducing a precision parameter $\epsilon \geq 0$, one can reformulate the SDP in (5.2) as feasibility problem with *threshold objective value* $\gamma \in \mathbb{R}$:

$$(5.5) \quad \begin{aligned} &\text{find} && H \in \mathbb{R}^{n \times n} \\ &\text{subject to} && \text{tr}(C\rho_H) - \frac{\gamma}{n} < \epsilon \|C\| \\ &&& \sum_{i=1}^n \left| (\rho_H)_{ii} - \frac{1}{n} \right| < \epsilon, \end{aligned}$$

where $\|\cdot\|$ denotes the operator norm. We can approximately determine the minimal threshold objective value $\gamma^* \in [-n\|C\|, n\|C\|]$ of (5.2) via a binary search. Here, the task of HU is to either find an H that fulfills both constraints in (5.5), or prove that no feasible H exists for a given value of γ . We can transform a feasible solution for the SDP relaxation (5.5) to a solution of the Ising problem (5.1) by applying randomized rounding as shown in (5.3). This means, we retrieve a feasible solution vector to the original Ising formulation and additionally an upper bound to the optimal value. Conversely, if γ is infeasible for the SDP relaxation (5.5), it inherently serves as a lower bound for the Ising problem (5.1), as given from the nature of relaxations. We can convert both, upper and lower bounds, for the Ising problem to bounds for the QUBO (2.1), and thus also for the original IP (3.1) and IQP (3.10), by reversing the steps of Appendix C.

The HU algorithm is an iterative process, where in each step one estimates the violation of the constraint (5.5) and updates H accordingly. We detect infeasible instances based on principles from quantum statistical mechanics involving an upper bound on the *relative entropy distance* between the initial Gibbs state $\rho_0 = \mathbb{1}_{n \times n}/n$ and a possible feasible solution state $\rho^* \in \mathbb{R}^{n \times n}$. To check the constraints, the matrix exponential $\exp(-H)$ needs to be computed in each iteration of HU, which is by far the most expensive part of the algorithm. Here, *quantum convex optimization* comes into play [BS17]. The central idea is to read (5.4) as a *physical* procedure, where H is a Hamiltonian operator and ρ_H a thermal quantum state. The problem of preparing such a Gibbs state given a classical description of the Hamiltonian is a well-studied problem in quantum computing [vAGGdW20]. This idea can be turned into a quantum algorithm for HU, with running time $\tilde{O}(n^{1.5}s^{0.5}\epsilon^{-5})$, compared to $\tilde{O}(\min\{n^3\epsilon^{-2}, n^2s\epsilon^{-3}\})$ for a classical implementation, where n refers to the size of the matrix $H \in \mathbb{R}^{n \times n}$, s denotes the maximal number of non-zero entries in the matrix and ϵ is the precision as defined in (5.5). For the details, see [HTO⁺25].

6. EXPERIMENTAL RESULTS

In the upcoming Section 6, we compare the SOS-SDP relaxation, see Section 4, and Hamiltonian Updates, see Section 5, computationally. We apply the SDP relaxations of both approaches to the QUBOs that we derive from the IP/IQP formulations of the problem instances from Subsections 3.1.1 and 3.2.1. As benchmark values for comparison, we provide the optimal values of the respective IPs/IQPs as well as the optimal/approximate values to the QUBO formulations by standard solvers, see Subsections 6.2.1 and 6.2.2.

6.1. **Experimental Setup.** We give a technical overview on our hardware and software setup:

- **Hardware and system information:** We use Ubuntu 18.04.6 LTS with an Intel(R) Core(TM) i7-8700 CPU @ 3.20GHz processor, six cores and two threads per core and 15GB of RAM by default for all computations. We compute selected examples using HU on an Nvidia Geforce RTX 4090 GPU.
- **Code and data availability:** We provide our data and executable scripts via https://moto.math.nat.tu-bs.de/appliedalgebra_public/sdp_qubo_benchmarking.
- **Software:** We derive the QUBO formulations via the GAMS QUBO_SOLVE tool available at <https://github.com/GAMS-dev/qubo>. Additionally, we use GAMS to provide IP/IQP solutions and QUBO solutions via the standard solvers CPLEX [Cpl09] and GUROBI [Gur24]. For the SDP relaxations based on SOS we rely on several academic and commercial software [WML19, WLC⁺19, ApS24, GCG21, HKS24, WH24, OCPB23]. For Hamiltonian Updates, we use the implementation introduced in [HTO⁺25] and available at <https://zenodo.org/records/14871936>.

6.1.1. **Instances.** As laid out in detail¹ in Subsections 3.1.2 and 3.2.2, we consider two OVRP instances emerging from an IP that we denote by OVRP11 and OVRP15 respectively, as well as three ASP instances, emerging from an IQP, that we denote by ASP30, ASP60 and ASP90. For the latter instances, we use multiple different penalties in the QUBO formulation to construct multiple QUBOs in order to explore if and how the penalties influence the solution of the SDP. We distinguish the different QUBOs emerging from the same IQP by a suffix to their name with the respective penalty. We give an overview over the five instances in Table 3.

	ASP			OVRP	
Instance	ASP30	ASP60	ASP90	OVRP11	OVRP15
QUBO Matrix size	$n = 96$	$n = 186$	$n = 276$	$n = 1750$	$n = 3380$
Sparsity	49.9%	53.5%	56.3%	92.2%	93.5%
Number of QUBOs	14	4	3	1	1

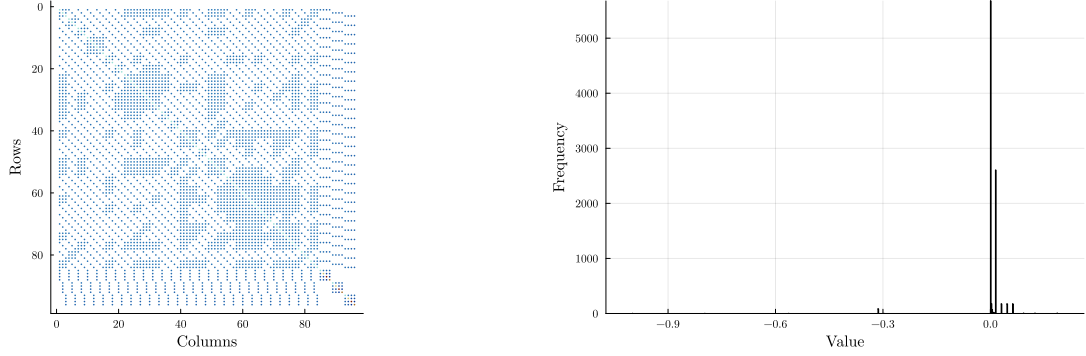
TABLE 3. Overview on the five **problem instances**. We display the size of the matrix $Q \in \mathbb{R}^{n \times n}$ and the sparsity as percentage of zero elements in Q after the QUBO reformulation. For the ASP instances, we each provide multiple QUBO formulations that differ by penalties used in the construction.

The OVRP instances are very large with matrix sizes $n = 1750$ and $n = 3380$ respectively, yet relatively sparse with each over 92% of zero entries. However, this yields still 238350 non-zero elements for OVRP11 and 740864 non-zero elements for OVRP15. Based on analyzing the singular values, the QUBO matrices of OVRP11 and OVRP15 are of relatively high rank, with numerical ranks of 1480 and 3002, respectively.

The ASP instances are smaller with $n = \{96, 186, 276\}$ and all have full numerical rank. Moreover, in each matrix about half of the entries are not zero. Note that the penalties in the QUBO formulation do not change the number nor position of the non-zero elements. Thus, the value for sparsity for each version of the QUBOs emerging from the ASP instances is the same.

¹In particular, the QUBOs we consider have a constant offset $c \in \mathbb{Z}$, depending on the penalty from the QUBO reformulation. Thus, for a symmetric matrix $Q \in \mathbb{R}^{n \times n}$, we tackle the problem $\min_{\mathbf{x} \in \{0,1\}^n} \mathbf{x}^T Q \mathbf{x} + c$. This problem differs from our initial definition by the offset c . However, since c does not alter the minimizer, we first solve a QUBO of the form (2.1) and later add c to the solution.

In Figure 2 we exemplarily show the sparsity pattern of the matrix entries for ASP30 with penalty 250, along with a histogram of the entries. It is visible that the entries are not normally distributed. In the display, all matrix entries are divided by the maximal absolute value.



(A) Sparsity Pattern for ASP30-250, all dots resemble a non-zero entry.

(B) Histogram of the distribution of matrix entries ASP30-250.

FIGURE 2. **Sparsity and distribution of non-zero entries** of the matrix corresponding to QUBO ASP30-250. All values are scaled by dividing with the largest entry of absolute value. The largest values by absolute value lie on the diagonal, this is indicated by different colors on the diagonal.

6.1.2. Attributes for comparison. In this section we introduce the different attributes that we use to compare the SOS-SDP methods and Hamiltonian Updates. While both approaches are SDP relaxations of the given QUBO they contain specific features that are not directly comparable. With the goal in mind of benchmarking SDP relaxations for QUBO formulations from a practitioner’s perspective on the specific given problem instances, we choose to compare in general two attributes that we attain from both approaches.

We label the *optimal value* of the ASP in the IQP formulation in Equation (3.10) as Z_{ASP}^* and the *optimal value* of the OVRP in the IP formulation in Equation (3.1) as Z_{OVRP}^* . For simplicity, we refer to both optimal values of ASP and OVRP as Z^* .

- **Lower bound:** Both SDP relaxations via SOS and HU provide a *lower bound* Z_{SOS} and respectively a *lower bound* Z_{HU} to the optimal value² Z^* . That means, we have $Z_{SOS}, Z_{HU} \leq Z^*$. In order to evaluate the quality of the lower bounds Z_{SOS} and Z_{HU} and compare them among each other, we state their distance to the optimal value Z^* . We do this via the *absolute differences* Δ_{SOS}^{abs} and Δ_{HU}^{abs} , denoted by

$$\Delta_{SOS}^{abs} = |Z_{SOS} - Z^*| \text{ and } \Delta_{HU}^{abs} = |Z_{HU} - Z^*|,$$

and via the *relative differences* Δ_{SOS}^{rel} and Δ_{HU}^{rel} to the optimal value Z^* , denoted by

$$\Delta_{SOS}^{rel} = \frac{\Delta_{SOS}^{abs}}{Z^*} \text{ and } \Delta_{HU}^{rel} = \frac{\Delta_{HU}^{abs}}{Z^*}.$$

²Both relaxations provide a lower bound to the optimal QUBO value. The QUBO is a reformulation of the corresponding IP/IQP with the same optimal value Z^* . The specific optimal values Z^* for our problem instances are positive and displayed in Table 4.

- **Running Time:** We record the running times t_{SOS} and t_{HU} respectively of each SDP relaxation that is spent to provide the above lower bounds Z_{SOS} , Z_{HU} .

Each approach provides multiple different parameters that influence the quality of the lower bounds as well as the running time. These parameters are individual to each approach. Likewise, we collect additional data that is not directly comparable to the other approach. We briefly describe these features for both methods:

Additional parameters and tracked data for SOS-SDP:

- The SOS hierarchy as in (4.4) provides a sequence of lower bounds to the optimal value, depending on the degree $2d$ of the corresponding polynomials. In our experiments, we perform first order relaxations ($2d = 2$) and second order relaxations ($2d = 4$) if possible due to the size of the corresponding SDP.
- As laid out in Subsection 4.3, we use different polynomial optimization software as well as internal SDP solvers.
- Note that a solution recovery for the SOS methods, i.e., attaining the vector $\mathbf{x}^* \in \{0, 1\}^n$, is only guaranteed if the optimal value is reached within the hierarchy, see e.g. [HL05, Lau09]. In our experiments we do not reach the optimal value.

Additional parameters and tracked data for HU:

- As described in Section 5, a crucial parameter in Hamiltonian Updates is the precision ϵ of the feasibility problem (5.5). For a high precision, the running time increases accordingly. In our experiments, we test values of ϵ in $\{10^{-2}, 10^{-3}, 10^{-4}\}$.
- The quantum version of HU gives an approximate number of quantum CNOT gates that would be used to perform the algorithm on a quantum computer, see [HTO⁺25] for further details on the gate count. We assume the current best time of $6.5 \times 10^{-9}s$ that could physically be realized to perform an isolated quantum gate operation [CTM⁺22] and multiply by the approximate number of CNOT gates. This gives an optimistic approximation of the running time $t_{HU}^{Quantum}$ of the SDP relaxation via HU on a quantum computer.
- The HU implementation provides the opportunity to be executed on a GPU via cudy [OUN⁺17] if available instead of the default CPU. Execution on GPU is faster.
- The randomized rounding procedure of Hamiltonian Updates, see (5.3), yields an approximate solution vector $\mathbf{x}_{HU} \in \{0, 1\}^n$ that provides an *upper bound* \tilde{Z}_{HU} to the optimal value Z^* . We define the absolute difference $\tilde{\Delta}_{HU}^{abs}$ and relative difference $\tilde{\Delta}_{HU}^{rel}$ to the optimal value Z^* , respectively, as

$$\tilde{\Delta}_{HU}^{abs} = |\tilde{Z}_{HU} - Z^*| \text{ and } \tilde{\Delta}_{HU}^{rel} = \frac{|\tilde{Z}_{HU} - Z^*|}{Z^*}.$$

We execute all SDP relaxations with the parameters as described above. Since we try to take a view point of a practitioner's perspective, we generally enforce time limits for the computations and stop them accordingly, see Table 11 in the appendix for details.

6.2. Benchmarks from IP/IQP and QUBO formulations.

6.2.1. Optimal IP/IQP solutions. We compute the optimal values Z^* of the OVRP with its IP formulation in (3.1) and the ASP with its IQP formulation in (3.10) via the standard solver CPLEX, see Subsection 6.1. The optimal values solve as benchmark for the SDP relaxations of the QUBO formulations. In Table 4 we provide the optimal values along with the corresponding

running times. The ASP problems are solved to optimality within a few seconds. The OVRP11 problem is solved to optimality within about two minutes, and OVRP15 under 20 minutes.

Instance	ASP30	ASP60	ASP90	OVRP11	OVRP15
Optimal value Z^*	246.78	820.08	1373.15	6254.19	3036.54
Running time CPLEX in s	0.45	2.07	2.82	123.81	1128.14

TABLE 4. Running times and optimal values Z^* to IP and IQP formulations for the OVRP and ASP problems, respectively, using CPLEX.

The standard methods for IPs/IQPs implemented in solvers such as CPLEX are highly optimized for solving exactly this type of problem formulation [JLN⁺10], yielding fast running times for these problems, see Table 4. This is the result of decades of development and refinement, specifically tailored to these types of problems [KBPV22]. Moreover, we emphasize here, that the corresponding problem instances were chosen such that their IP/IQP formulation is solvable to optimality providing a benchmark for comparisons.

6.2.2. QUBO Solver Results. The QUBO reformulation, see Subsection 3.3, changes the problem type from IP/IQP to QUBO, even though the optimal value Z^* is the same. In the upcoming sections we compare different SDP relaxations of these QUBO formulations and use the optimal value Z^* as a benchmark. Thus, for completeness, in the remainder of this subsection, we try to solve the QUBO formulations to optimality. We point out that the QUBO reformulation is more difficult to solve than the original IP/IQP formulations due to the increased number of auxiliary binary variables, which in turn expand the search space of the problem, see [GRS24]. Moreover, the penalty term in the QUBO formulation plays a significant role in the optimization process, see Appendix A.2.2, [KHG⁺14] and [ARCR⁺24].

For reference and comparison with our goal of benchmarking the SDP relaxations, we provide the solutions to the QUBO formulation that we obtain from quadratic solvers implemented in CPLEX and GUROBI. There exists more specialized academic software such as BIQMAC [RRW10], BIQCRUNCH [KMR17], MADAM [HP21], BIGBIN [GHL⁺22] as well as QUBOWL [RKS23] and MCSPARSE [CJMM22] for large sparse problems, specifically designed for solving QUBOs. For the scope of this paper, we chose the quadratic solver included in CPLEX and GUROBI to serve as benchmark of QUBO solvers and direct the reader to the above articles for detailed comparisons of the QUBO solvers. Some of the solvers are only available as web services and on many benchmark instances used in [RKS23] the commercial solver GUROBI outperforms them.

Whereas for the IP/IQP formulations the solver stops with proven optimality, for the QUBO formulation we have to stop the solving process at a certain imposed time limit. Then we verify whether the constraints are satisfied by substituting the solution into the original problem and assess its optimality by comparing the objective value of the QUBO to Z^* .

We denote the objective value reached by solving the QUBO formulation after a certain time limit as p_{QUBO} . This is an **upper bound** to Z^* . In Figure 3, we exemplarily display Z_{QUBO} that we obtain for the ASP30 instances with a time limit of 120 s with the solver CPLEX. For the penalties 400, 500 and 550, optimality is reached. Note that this is an upper bound for the time needed to reach the optimal value. For the other instances we find feasible solutions, but not the optimal one, after 120 s. We see here that the chosen penalty in the QUBO construction influences the result significantly.

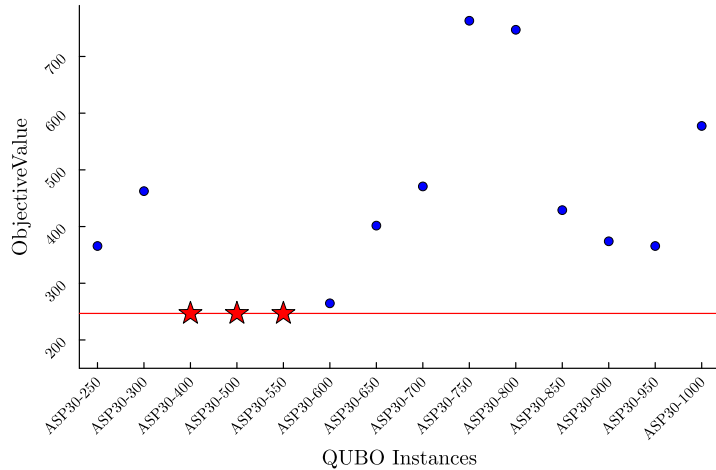


FIGURE 3. **Objective values** Z_{QUBO} for solving the **QUBO formulations** of ASP30 with **different penalties** using CPLEX and a **time limit of 120 seconds**. The red line indicates the optimal value Z^* of ASP30. The blue dots are the objective values Z_{QUBO} , additionally the red stars indicate that the optimal value was reached for these formulations.

We denote the absolute difference of the upper bound Z_{QUBO} to the optimal value Z^* and by the relative difference, respectively, by:

$$\Delta_{\text{QUBO}}^{\text{abs}} = |Z_{\text{QUBO}} - Z^*| \text{ and } \Delta_{\text{QUBO}}^{\text{rel}} = \frac{\Delta_{\text{QUBO}}^{\text{abs}}}{Z^*}$$

For ASP60 and ASP90, we find feasible solutions after a set time limit of 120s using CPLEX. However, these upper bounds are very large, e.g. the relative difference to the optimal value is $\Delta_{\text{QUBO}}^{\text{rel}} > 1300\%$ for ASP90-1450, meaning that the upper bound is by a factor of 13 larger than the optimal value. For the OVRP instances, we did not obtain a feasible solution after setting the time limit to 30 minutes using CPLEX. This indicates the difficulty of the QUBO formulation compared to the IP/IQP formulations that we could solve to optimality, see Table 4.

We additionally try to tackle the problems via the standard solver GUROBI [Gur24] that produces better solutions for the larger instances ASP60 and ASP90. We give an exemplary overview on $\Delta_{\text{QUBO}}^{\text{rel}}$ for different time limits in Table 5, see Table 15 for $\Delta_{\text{QUBO}}^{\text{abs}}$ correspondingly.

Instance	Time Limit	$\Delta_{\text{QUBO}}^{\text{rel}}$	Time Limit	$\Delta_{\text{QUBO}}^{\text{rel}}$	Time Limit	$\Delta_{\text{QUBO}}^{\text{rel}}$
ASP30-950	10s	0	120s	0	600s	0
ASP60-900	10s	0.29	120s	0.29	600s	0.29
ASP90-1450	10s	0.40	120s	0.21	600s	0.19

TABLE 5. **Relative difference** $\Delta_{\text{QUBO}}^{\text{rel}}$ of the upper bound Z_{QUBO} to the optimal value for selected **QUBOs** using GUROBI with different time limits. For ASP30-950 we find the optimal value. The provided time limits are upper bounds on the running time to reach the respective objective value Z_{QUBO} . The computation is stopped at the provided time limit.

In particular, for the instance ASP60-900, we have $\Delta_{\text{QUBO}}^{\text{rel}} \approx 29\%$. Comparing to Figure 3, different penalties work well on GUROBI. While we only find a feasible, but not optimal solution for ASP30 with penalties $\{400, 500, 550\}$, we find an optimal solution for ASP30-950.

Similarly to CPLEX, GUROBI does not provide feasible solutions for either OVRP instance within a time limit of 30 minutes. For reference, in Appendix E.4, we exemplarily provide results using the D-Wave’s Quantum Annealer Procedure that we access via GAMS’s QUBO_SOLVE tool, see Subsection 6.1. Similarly, we find the optimal solution for ASP30, and feasible solutions for ASP60 and ASP90 but the OVRP instances give infeasible solutions.

6.3. Experimental Results of SDP relaxations. In the following Subsections 6.3.1 and 6.3.2 we provide the results of the SDP relaxations concerning the larger QUBOs emerging from the OVRPs and from the smaller QUBOs from the ASPs, respectively. We tackle these QUBOs via the SOS-SDP relaxations from Section 4 and HU from Section 5.

6.3.1. SDP relaxations of QUBO formulations for OVRP. In Table 6 we summarize the results of the SDP relaxations for the QUBOs constructed from the OVRPs for SOS-SDP and HU methods.

	OVRP11			OVRP15		
	$\Delta_{\text{SOS}}^{\text{rel}} \Delta_{\text{HU}}^{\text{rel}}$	$t_{\text{SOS}} t_{\text{HU}}$ in s	$t_{\text{HU}}^{\text{Quantum}}$ in s	$\Delta_{\text{SOS}}^{\text{rel}} \Delta_{\text{HU}}^{\text{rel}}$	$t_{\text{SOS}} t_{\text{HU}}$ in s	$t_{\text{HU}}^{\text{Quantum}}$ in s
SOS.JL	†	†	-	†	†	-
TSSOS	†	†	-	†	†	-
MANISDP	1.32	28.08	-	1.60	95.63	-
HU $_{\epsilon=10^{-2}}$	7.9×10^6	58.01	9.3×10^{12}	5.6×10^7	310.36	9.4×10^{12}
HU $_{\epsilon=10^{-3}}$	7.4×10^5	348.02	3.3×10^{18}	6.2×10^6	1314.95	2.0×10^{18}

TABLE 6. **Results of SDP relaxations** of QUBOs referring to OVRP11 and OVRP15 comparing SOS and HU methods. Rows for SOS methods are gray, rows for HU methods are white. We display relative differences of the lower bounds to the optimal value by $\Delta_{\text{SOS}}^{\text{rel}}$ and $\Delta_{\text{HU}}^{\text{rel}}$, respectively, as well as running times for solving the SDP by t_{SOS} and t_{HU} , respectively, depending on the method, indicated by ‘|’. Note that $t_{\text{HU}}^{\text{Quantum}}$ is not available for SOS methods, as indicated by ‘-’. A dagger ‘†’ indicates that no result is available due to solver break down or exceeding maximal running time.

SOS-SDP. From both SOS.JL and TSSOS we do not receive a result for any of the QUBOs resulting from OVRP11 and OVRP15. We stop COSMO inside TSSOS after four hours for OVRP11. All internal SDP solvers, i.e., MOSEK and LORAINÉ, as well as SCS break down for the first order relaxation.

Using ManiSDP we are able to execute the first order relaxation for both problems and produce a lower bound within approximately 0.5 and 1.5 minutes, that still yield a relative difference $\Delta_{\text{SOS}}^{\text{rel}}$ of more than 100% of the optimal IP values Z^* . These results from MANISDP are the only benchmarks we achieve on the SOS side, concerning the OVRP instances.

HU. We execute HU for the precision ϵ in $\{10^{-2}, 10^{-3}\}$ and produce lower bounds Z_{HU} in a few minutes for OVRP11, and in about 20 minutes for OVRP15, using $\epsilon = 10^{-3}$. Translated to the quantum version of HU, based on the assumptions in Subsection 6.1.2 and [HTO⁺25] it would

	OVRP11			OVRP15		
	$\Delta_{\text{HU}}^{\text{rel}}$	t_{HU} in s	$t_{\text{HU}}^{\text{Quantum}}$ in s	$\Delta_{\text{HU}}^{\text{rel}}$	t_{HU} in s	$t_{\text{HU}}^{\text{Quantum}}$ in s
$\text{HU}^*_{\epsilon = 10^{-2}}$	7.9×10^6	12.51	9.3×10^{12}	5.6×10^7	72.64	9.4×10^{12}
$\text{HU}^*_{\epsilon = 10^{-3}}$	7.4×10^5	68.83	3.3×10^{18}	6.2×10^6	266.42	2.0×10^{18}
$\text{HU}^*_{\epsilon = 10^{-4}}$	7.1×10^4	16578.44	2.3×10^{24}	5.5×10^5	37405.86	4.7×10^{24}

TABLE 7. **Results of SDP relaxations via HU** of QUBOs referring to OVRP11 and OVRP15. In contrast to Table 6 these results are obtained via execution on a GPU, indicated by '*' for distinction. Running times t_{HU} are marked bold.

take more than 10^{10} years to solve the SDP on a quantum computer with $\epsilon = 10^{-3}$ for both problems. Even then, the lower bounds achieved are extremely far away from the optimal value.

The above results for HU are performed on a CPU. Using a GPU, we can accelerate the running time t_{HU} of the classical HU version such that we can use smaller tolerances ϵ in a reasonable time frame. We present the corresponding results in Tables 7 and 13.

We see that the GPU decreases running times significantly. However, solving OVRP15 with $\epsilon = 10^{-4}$ takes approximately 10 h with a relative difference $\Delta_{\text{HU}}^{\text{rel}} \approx 5.5 \times 10^5$ of the lower bound Z_{HU} to the optimal value. Through the randomized rounding procedure in HU, we also produce upper bounds \tilde{Z}_{HU} that are closer to the optimal value, e.g. we have $\tilde{\Delta}_{\text{HU}}^{\text{rel}} \approx 2.2 \times 10^4$ for OVRP15 at $\epsilon = 10^{-4}$. Nevertheless, this is still very far from the optimal value.

We summarize that the QUBOs derived from the OVRPs are too large to be tackled via the SDP solvers within the SOS methods. While we can at least solve the problem with MANISDP within 0.5 to 1.5 min, the second order relaxation of the Lasserre hierarchy cannot be executed, leaving still a large relative difference $\Delta_{\text{SOS}}^{\text{rel}}$ to the optimal value. The HU method can tackle the large problem producing lower and upper bounds but for reasonable running times only with low precision.

6.3.2. SDP relaxations of QUBO formulations for ASP. Compared to the OVRP instances, the ASP instances can be tackled by the SOS-SDP methods. We first describe the results for the SOS-SDP methods and afterwards for HU.

SOS-SDP. We give an overview on the most promising results in Table 8, see also Table 12 in the appendix, by presenting the average over the relative differences $\Delta_{\text{SOS}}^{\text{rel}}$ and running times t_{SOS} over each set ASP30, ASP60 and ASP90 with different penalties, respectively.

In particular, we are able to receive solutions for a range of methods on the smallest instance ASP30. In Figure 4, we show the relative difference $\Delta_{\text{SOS}}^{\text{rel}}$ to the optimal value obtained by different solvers for each penalty. This display resembles the first order Lasserre relaxation with a relative difference to the optimal value of $\Delta_{\text{SOS}}^{\text{rel}} > 100\%$ for almost all solvers and instances. Interestingly, the lower bounds improve slightly with a higher penalty in the QUBO formulation. We observe that using the default parameters in MOSEK, LORAINE and MANISDP, we get the same lower bounds. We note that, while MOSEK reports a FEASIBLE_POINT, LORAINE reports an UNKNOWN_RESULT_STATUS for these bounds. The fastest solver is ManiSDP with an average solving time of about 1.5s for all ASP30 instances. The solver COSMO inside TSSOS does *not* output a lower bound for any instance, the SCS solver on the Ising formulation does not reliably give lower bounds for all penalties, using the default settings.

	ASP30		ASP60		ASP90	
	Average $\Delta_{\text{SOS}}^{\text{rel}}$	Average t_{SOS}	Average $\Delta_{\text{SOS}}^{\text{rel}}$	Average t_{SOS}	Average $\Delta_{\text{SOS}}^{\text{rel}}$	Average t_{SOS}
MANISDP	1.99	1.45s	3.01	0.82s	2.41	1.45s
SOS.JL w. MOSEK	1.99	9.91s	3.01	221.25s	2.41	8256.9s
SOS.JL w. LORAINE	1.99	670.66s	†	†	†	†
TSSOS w. MOSEK	1.99	3.24s	3.01	112.42s	†	†
TSSOS w. MOSEK	0.13	28.46s	0.21	912.47s	†	†

TABLE 8. **Results of SOS-SDP relaxations** of QUBOs referring to ASP30, ASP60 and ASP90. We display the **average** of the relative difference $\Delta_{\text{SOS}}^{\text{rel}}$ to the optimal value and running times t_{SOS} for each set of instances. The gray row refers to the second order Lasserre relaxation, the other rows refer to the first order relaxation. A dagger '†' indicates that no result is available due to solver break down or exceeding maximal running time. For MOSEK, we display the result with the default tolerance $\text{tol}=10^{-8}$. For SOS.JL with MOSEK the total solving time of all ASP90 instances exceeds our set time limit. We display a rerun for these instances without time limit.

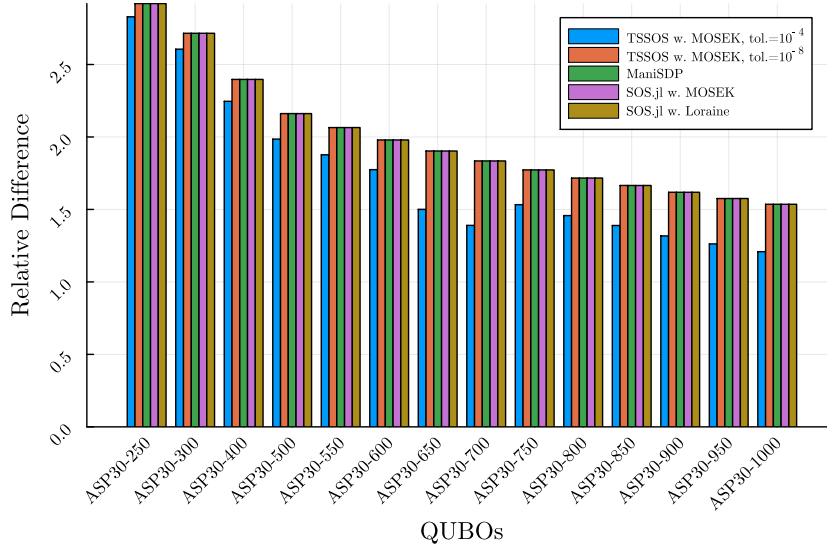


FIGURE 4. Relative Difference $\Delta_{\text{SOS}}^{\text{rel}}$ on all ASP30 instances with different penalties, obtained with **first order** relaxations, $2d = 2$.

For ASP30, we are able to execute the second order Lasserre relaxation via TSSOS and the solver MOSEK³. We display the results for two different parameter settings in Figure 5. The second order relaxation provides close lower bounds to the optimal value: On average, we

³Both MANISDP and TSSOS with COSMO can also execute the second order relaxation, however the results are not promising: COSMO does not yield lower bounds and MANISDP reaches lower bounds with $\Delta_{\text{SOS}}^{\text{rel}}$ of order 10⁵% in an hour of running time. Using MOSEK and COSMO inside SOS.JL, the solver breaks down for the second order relaxation.

can achieve a relative difference $\Delta_{\text{SOS}}^{\text{rel}} \approx 13\%$ ($\Delta_{\text{SOS}}^{\text{abs}} \approx 32.7$) using TSSOS with MOSEK and $\text{tol} = 10^{-8}$ with a running time of 28.5s. We do not achieve a higher relaxation order. Note that we see from Figure 5 that we get slightly better bounds with a larger tolerance of $\text{tol} = 10^{-4}$, though these bounds are not certified as FEASIBLE_POINT in the solver output.

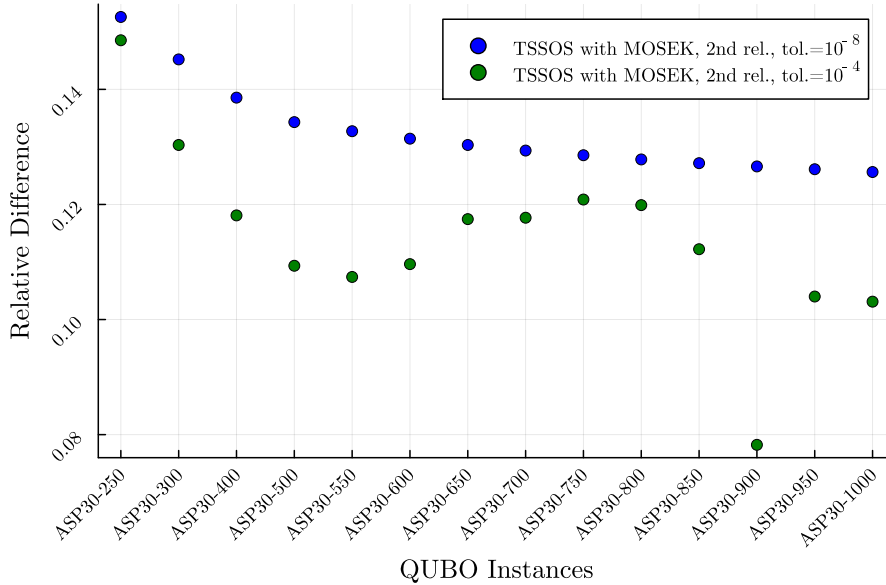


FIGURE 5. Relative Difference $\Delta_{\text{SOS}}^{\text{rel}}$ on all ASP30 instances with different penalties, obtained with **TSSOS**, using MOSEK with the **second order** relaxation, $2d = 4$ and the default tolerances of 10^{-8} , as well as 10^{-4} .

We give an overview on all ASP60 instances in Figure 6. We again receive the best lower bounds by running the second order relaxation with TSSOS using MOSEK. With the default tolerance, $\text{tol} = 10^{-8}$, this yields an average relative difference $\Delta_{\text{SOS}}^{\text{rel}}$ of 21% ($\Delta_{\text{SOS}}^{\text{abs}} \approx 174.3$) with a running time of over 15 minutes on average.

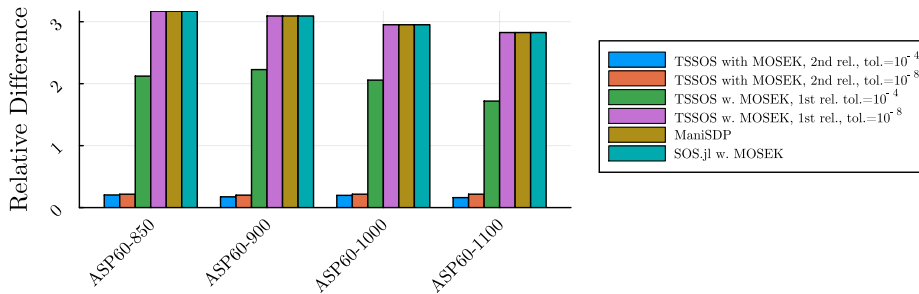


FIGURE 6. Relative Difference $\Delta_{\text{SOS}}^{\text{rel}}$ on ASP60 instances with different penalties.

However, for the larger ASP90 instances, we do not achieve any results with TSSOS, the internal solver MOSEK breaks down even for the first order relaxation. We can only tackle ASP90 via the first order relaxation inside SOS.JL using MOSEK and MANISDP. The former

yields an average relative difference $\Delta_{\text{SOS}}^{\text{rel}}$ of 240% ($\Delta_{\text{SOS}}^{\text{abs}} \approx 3308.5$) within an average running time t_{SOS} of over 2h while MANISDP achieves the same result in on average 1.5s.

HU. We display the relative differences of the lower bounds as well as the upper bounds obtained by the randomized rounding procedure for all ASP30 instances in Figure 7. We see that the upper bounds are closer to the optimal value than the lower bounds, yet still very far away. In particular, on average, the upper bounds to the optimal value yield $\tilde{\Delta}_{\text{HU}}^{\text{rel}} \approx 2700\%$ ($\tilde{\Delta}_{\text{HU}}^{\text{abs}} \approx 6688.7$) for precision $\epsilon = 10^{-3}$, while for the lower bounds, the average $\Delta_{\text{HU}}^{\text{rel}}$ is of order $10^4\%$. We notice that for our given instances, the upper and lower bounds improve with a decreasing penalty in the QUBO formulation. This can be explained by the fact that the precision of the HU solution gets scaled with the norm of the cost matrix C of the Ising problem (5.1). As larger penalties lead to a higher norm of C , consequently the gap between lower and upper bound becomes larger. Running the experiments on the default CPU, we produce these results within few seconds for $\epsilon = 10^{-2}$ and on average 57 s per instance for $\epsilon = 10^{-3}$.

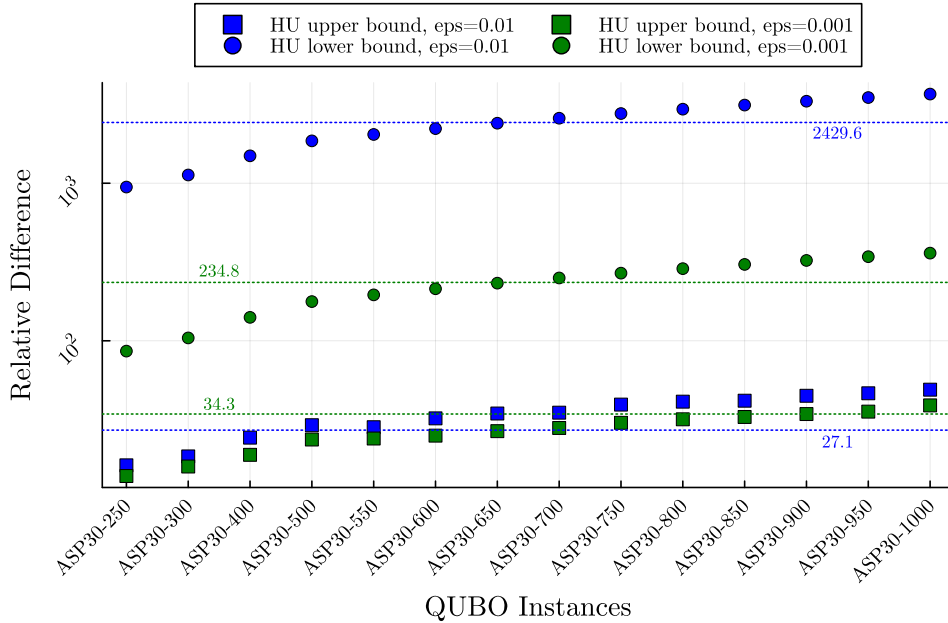


FIGURE 7. **Relative Differences** $\Delta_{\text{HU}}^{\text{rel}}$, $\tilde{\Delta}_{\text{HU}}^{\text{rel}}$ of **lower bounds** Z_{HU} and **upper bounds** \tilde{Z}_{HU} , respectively, to optimal value, on all ASP30 instances with different penalties, obtained with HU and precisions $\epsilon = 10^{-2}$ and $\epsilon = 10^{-3}$. Dotted lines display the average values for $\Delta_{\text{HU}}^{\text{rel}}$ and $\tilde{\Delta}_{\text{HU}}^{\text{rel}}$ over all ASP30 instances. The y -scale is logarithmic.

In Tables 9 and 10 we exemplarily compute the SDP relaxations via HU on a GPU for the instances ASP30-250, ASP60-850 and ASP90-1400. For this exemplary display, we choose the instances with the smallest penalty from the QUBO construction. The GPU provides faster results than the default CPU, letting us try smaller tolerances ϵ in a reasonable running time. With $\epsilon = 10^{-5.5}$, we receive a lower bound Z_{HU} for ASP30-250 that has a relative difference $\Delta_{\text{HU}}^{\text{rel}} \approx 310\%$, taking a classical running time of more than three days. To achieve this precision for ASP30-250 using the quantum version of HU would take an order of 10^{20} years.

	ASP30-250			
	$\Delta_{\text{HU}}^{\text{rel}}$	$\tilde{\Delta}_{\text{HU}}^{\text{rel}}$	t_{HU} in s	$t_{\text{HU}}^{\text{Quantum}}$ in s
$\text{HU}^*_{\epsilon = 10^{-2}}$	945.6	16.8	0.17	8.4×10^{10}
$\text{HU}^*_{\epsilon = 10^{-3}}$	86.0	14.2	3.08	1.2×10^{16}
$\text{HU}^*_{\epsilon = 10^{-4}}$	8.8	6.6	500.36	3.1×10^{21}
$\text{HU}^*_{\epsilon = 10^{-5}}$	3.8	3.2	21861.1	7.7×10^{25}
$\text{HU}^*_{\epsilon = 10^{-5.5}}$	3.1	2.8	2.7×10^5	3.5×10^{28}

TABLE 9. **Results of SDP relaxations via HU** of QUBOs referring to ASP30-250. These results are obtained via execution on a **GPU**, indicated by '*' for distinction. We display relative differences to optimum $\Delta_{\text{HU}}^{\text{rel}}$ and $\tilde{\Delta}_{\text{HU}}^{\text{rel}}$ of lower bounds and upper bounds, respectively.

	ASP60-850			ASP90-1400		
	$\Delta_{\text{HU}}^{\text{rel}}$	t_{HU} in s	$t_{\text{HU}}^{\text{Quantum}}$ in s	$\Delta_{\text{HU}}^{\text{rel}}$	t_{HU} in s	$t_{\text{HU}}^{\text{Quantum}}$ in s
$\text{HU}^*_{\epsilon = 10^{-2}}$	5.4×10^3	0.23	2.6×10^{11}	1.9×10^4	0.5	5.2×10^{11}
$\text{HU}^*_{\epsilon = 10^{-3}}$	807.5	3.98	4.2×10^{16}	2.7×10^3	4.99	6.7×10^{16}
$\text{HU}^*_{\epsilon = 10^{-4}}$	74.42	504.7	1.1×10^{22}	256.2	1313.8	5.8×10^{22}

TABLE 10. **Results of SDP relaxations via HU** of QUBOs referring to ASP60-850 and ASP90-1400. These results were obtained via execution on a **GPU**, indicated by '*' for distinction. See Table 14 for upper bounds.

We summarize our findings on both SOS and HU methods, displaying the ASP30 instances in Figure 8: The plot shows the average running times t_{SOS} and t_{HU} for several methods, while also indicating the relative differences $\Delta_{\text{SOS}}^{\text{rel}}$ and $\Delta_{\text{HU}}^{\text{rel}}$. Only via the second order Lasserre hierarchy with TSSOS using MOSEK, we could achieve $\Delta_{\text{SOS}}^{\text{rel}} < 20\%$. The fastest running times are performed by MANISDP and the classical version of HU with low precision.

6.4. Discussion. We highlight again that the goal of this study is not to suggest or promote a certain method but to compare existing methods for SDP relaxations on **real-world data**.

The parameter settings in the real-world applications are chosen with the intention to make the instances solvable for IP/IQP solvers and thus provide optimal benchmarks. As described in Section 3, the downside is that these settings yield the smallest instances to be encountered in industry. However, from the – for industry standards – small instances, we observe that the **QUBO formulations** of these problems are hard for all tested methods.

As expected, the standard solvers GUROBI and CPLEX optimally solve the IQP respectively IP formulations of the smaller ASP instances in seconds and the largest OVRP instance in under 20 minutes. As shown in the QUBO benchmarks by Mittelmann [Mit24], specialized QUBO solvers, see Subsection 6.2.2, can solve the QUBO instances from the QPLIB [FTB⁺18] library with up to 700 variables, and sparse instances even up to 10.000 variables [RKS23]. Especially, dense QUBO instances are often randomly generated [Wie07, RKS23, WH24, HKS24]. With the ASP instances, we provide QUBO formulations from real-world instances with about 50% non-zero entries. Recall, that the largest ASP instance ASP90 has 276 variables. Hence, merely based on the number of variables, it is expectable that the sizes of our instances are solvable for specialized QUBO solvers. We point out here, that our instances are not QUBO instances by

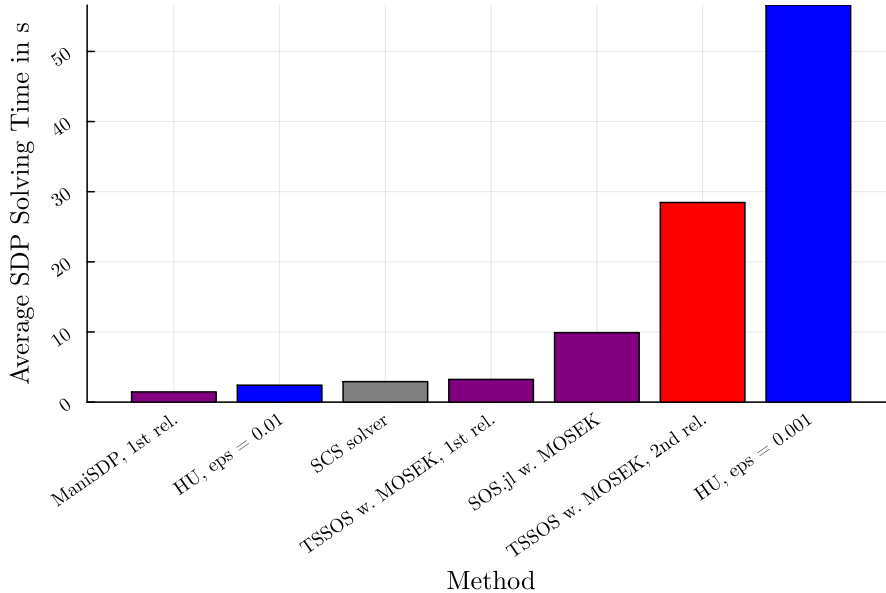


FIGURE 8. **Averages** over **running times** t_{SOS} and t_{HU} of all ASP30 instances for different methods. The red bar indicates that the average relative difference $\Delta_{\text{SOS}}^{\text{rel}} \leq 0.2$. The purple bars indicate that $\Delta_{\text{SOS}}^{\text{rel}} \leq 2$. The blue bars indicate that $\Delta_{\text{HU}}^{\text{rel}}$ is larger than 2. The gray bar indicates, that the solver did not output a reliable lower bound $\Delta_{\text{SOS}}^{\text{rel}}$. For TSSOS with MOSEK $\text{tol}=10^{-8}$ is displayed. If there is no other explicit description, the first order Lasserre relaxation is displayed for SOS methods. SOS.JL with LORAINE reached an average relative difference $\Delta_{\text{SOS}}^{\text{rel}} \approx 1.99$ but is not displayed due to average running time of $> 600s$. HU is executed on the default CPU.

nature nor MaxCut instances, and we reformulate their IP/IQP formulations to QUBOs. From Subsection 6.2.2, we see that, using standard solvers CPLEX and GUROBI, we can only solve the smaller instance ASP30 with 96 variables to optimality for certain penalties in the QUBO reformulation, while we obtain no feasible solution for the OVRP instances. While we do not use the specialized solvers in the scope of this paper, we see the difficulty of the reformulated problems from the behavior of the standard solvers.

The focus on our paper lies on Subsection 6.3, where we relax the QUBO formulations and provide lower bounds to the optimal value. Using the **SOS-SDP** approach, we test several software from polynomial optimization. As expected, we observe that the SDP solvers in their default settings do not always return reliable solutions, see e.g. [SWW21], do not output lower bounds to the optimal values, or even break down given the size of the SDPs. The software TSSOS with internal SDP solver MOSEK provides the qualitatively best lower bound for the smallest problems ASP30 and ASP60 with an relative difference to the optimal value of 13% and 21% respectively, performing the second Lasserre relaxations. However, we cannot tackle the larger problems and higher relaxations. Using the other SOS-SDP methods, we can only provide the first order relaxations that give lower bounds with relative differences to the optimal value of $\gg 100\%$ for the tested instances. In terms of running time, the SDP solver MANISDP is very

fast and finds these bounds in very few seconds for the ASP instances, as well as being the only tested SOS-SDP method that gives results for the OVRP instances, within only 1.5 minutes.

Hamiltonian Updates is an algorithm that scales in favor of the matrix input size, providing the opportunity to solve very large SDPs. However, this comes with a costly dependence of the running time with the precision. As expected, we can solve all instances via HU within seconds or few minutes for a low precision. However, on the tested instances, we can only give very poor lower bounds to the optimal value, where the best achieved relative differences to the optimal values is still $\gg 300\%$.

The running time of the quantum version of HU can be approximated via counting the quantum gates in an optimistic way, in favor of the physical realization of a quantum computer. We see, however, that the approximated running times exceed its classical version tremendously on our tested instances, see [HTO⁺25] for a non-asymptotic analysis of the running time, showing that the quantum approach does not beat the classical version on realistic instances despite asymptotical advantage.

Using the randomized rounding procedure, we furthermore get upper bounds to the optimal value, as well as a feasible solution vectors. While these upper bounds are also far away from the optimal values, it is an advantage over most current implementations of SOS-SDP methods, where solutions extraction is based on the Fialkow-Curto approach, which is only guaranteed to be applicable if the hierarchy converges to the optimal value; see e.g. [Lau09].

7. CONCLUSION

It is widely known that in optimization real-world data behaves differently than randomly generated data, which is often used in the development of algorithms and software. In this work, we make the same observation. We see moreover that reformulating IP/IQP problems to QUBOs increases the difficulty of the instances if they are not naturally QUBO or MaxCut instances. Our test instances are by far best solved by the specialized and well-developed IP/IQP methods.

The goal of this work was to compare SDP relaxations of QUBO formulations stemming from real-world IPs/IQPs. We see that we can solve the smallest QUBOs directly, using quadratic solvers of GUROBI and CPLEX, and still achieve better lower bounds than with the first order SOS-SDP relaxations and the SDP relaxation via HU. If only comparing the SDP approaches, we observe that on the chosen instances the quality of the lower bounds provided by SOS-SDP is better than using HU.

While on the tested instances the quality of solutions is non-competitive, HU can provide lower bounds to very large problems, where SOS-SDP methods and QUBO solvers fail, and it also gives upper bounds and feasible solutions. Generally, the practitioner needs more than just a lower bound on the solution – i.e., an actual solution to the optimization problem is needed, or at the very least, upper and lower bounds. Even though HU scales unfavorably with high precision, it does provide these properties. Therefore, it would be interesting to conduct further research on its applicability to large real-world instances.

In general we notice that also on the polynomial optimization side, the results are very much dependent on the method and the solver. Especially, approaches exploiting sparsity perform well in our experiments, directing the future research to more specialized solvers and software for preprocessing specifically considering the structure and properties of the problem. With this work, we confirm the trend that developing these methods is fruitful, as well as testing them not only on randomly generated data.

8. ACKNOWLEDGMENTS

All authors were supported by the German Federal Ministry for Economic Affairs and Climate Action (BMWK), project ProvideQ. FH and DG are also supported by the German Federal Ministry of Education and Research (BMBF), project QuBRA and by Germany’s Excellence Strategy – Cluster of Excellence Matter and Light for Quantum Computing (ML4Q) EXC 2004/1 (390534769). We thank Sabrina Ammann for helpful comments on the draft, as well as Jie Wang, Victor Magron, Amir Ali Ahmadi and Christoph Helmberg for insightful discussions.

9. AUTHORS’ CONTRIBUTIONS

TG, WG, FF, TdW and DG initiated the project. TdW lead the project and coordinated it jointly with BO. TdW, DG, FF and WG supervised the project locally in the respective research groups. BO, FH and VJ carried out the implementation of the different methods, ran preliminary experiments and conceptualized the experimental study, AD assisted them. AD implemented unifying scripts of the codes to run the experiments. BO, FH, VJ evaluated the results and TdW, DG, FF and TG gave feedback on the results. AD, BO, VJ and FH wrote the code documentation. BO, TG, VJ, FH and TdW wrote the initial draft of the manuscript. BO visualized the experimental results. JN modeled the ASP formulation and processed the original ASP data. TdW and BO revised and edited the draft with support of TG, VJ and FH. All authors revised the final manuscript.

REFERENCES

- [AA00] Erling D. Andersen and Knud D. Andersen. The mosek interior point optimizer for linear programming: an implementation of the homogeneous algorithm. In *High performance optimization*, pages 197–232. Springer, 2000.
- [ABCC] David Applegate, Ribert Bixby, Vasek Chvatal, and William Cook. Concorde TSP solver. <http://www.math.uwaterloo.ca/tsp/concorde>. Accessed 01/24.
- [AHR⁺23] Sabrina Ammann, Maximilian Hess, Debora Ramacciotti, Sándor P. Fekete, Paulina L. A. Goedicke, David Gross, Andreea Lefterovici, Tobias J. Osborne, Michael Perk, Antonio Rotundo, S. E. Skelton, Sebastian Stiller, and Timo de Wolff. Realistic runtime analysis for quantum simplex computation, 2023.
- [AM16] Amir Ali Ahmadi and Anirudha Majumdar. Some applications of polynomial optimization in operations research and real-time decision making. *Optimization Letters*, 10(4):709–729, 2016.
- [AM19] Amir Ali Ahmadi and Anirudha Majumdar. Dsos and sdsos optimization: More tractable alternatives to sum of squares and semidefinite optimization. *SIAM Journal on Applied Algebra and Geometry*, 3(2):193–230, 2019.
- [ApS24] MOSEK ApS. *MOSEK Optimizer API for Julia Release 10.1.31*, 2024.
- [ARCR⁺24] Edoardo Alessandrini, Sergi Ramos-Calderer, Ingo Roth, Emiliano Traversi, and Leandro Aolita. Alleviating the quantum big- m problem. <https://arxiv.org/abs/2307.10379>, 2024.
- [AS25] Gennadiy Averkov and Claus Scheiderer. Convex hulls of monomial curves, and a sparse positivstellensatz. *Math. Prog.*, 209:113–131, 2025.
- [BMAS14] Nicolas Boumal, Bamdev Mishra, P.-A. Absil, and Rodolphe Sepulchre. Manopt, a Matlab toolbox for optimization on manifolds. *Journal of Machine Learning Research*, 15(42):1455–1459, 2014.
- [BMN⁺21] Ryan Babbush, Jarrod R. McClean, Michael Newman, Craig Gidney, Sergio Boixo, and Hartmut Neven. Focus beyond quadratic speedups for error-corrected quantum advantage. *PRX Quantum*, 2(1), March 2021.
- [BMPR09] Filippo Bindi, Riccardo Manzini, Arrigo Pareschi, and Alberto Regattieri. Similarity-based storage allocation rules in an order picking system: an application to the food service industry. *International Journal of Logistics: Research and Applications*, 12(4):233–247, 2009.
- [Bor17] Zuzana Borcinova. Two models of the capacitated vehicle routing problem. *Croatian Operational Research Review*, 8:463–469, 2017.

- [BS17] Fernando G.S.L. Brandao and Krysta M. Svore. Quantum speed-ups for solving semidefinite programs. In *2017 IEEE 58th Annual Symposium on Foundations of Computer Science (FOCS)*, pages 415–426, 2017.
- [Çel99] Eranda Çela. The quadratic assignment problem theory and algorithms. *Journal of the Operational Research Society*, 50(5), 1999.
- [CJMM22] Jonas Charfreitag, Michael Jünger, Sven Mallach, and Petra Mutzel. *McSparse: Exact Solutions of Sparse Maximum Cut and Sparse Unconstrained Binary Quadratic Optimization Problems*, pages 54–66. 2022.
- [CJY⁺22] Chin-Yao Chang, Eric Jones, Yiyun Yao, Peter Graf, and Rishabh Jain. On hybrid quantum and classical computing algorithms for mixed-integer programming, 2022.
- [CKM19] Earl Campbell, Ankur Khurana, and Ashley Montanaro. Applying quantum algorithms to constraint satisfaction problems. *Quantum*, 3:167, July 2019.
- [CLL12] Yi-Fei Chuang, Hsu-Tung Lee, and Yi-Chuan Lai. Item-associated cluster assignment model on storage allocation problems. *Computers & Industrial Engineering*, 63(4):1171–1177, 2012.
- [Cpl09] IBM ILOG Cplex. V12. 1: User’s manual for cplex. *International Business Machines Corporation*, 46(53):157, 2009.
- [CS16] Venkat Chandrasekaran and Parikshit Shah. Relative Entropy Relaxations for Signomial Optimization. *SIAM J. Optim.*, 26(2):1147–1173, 2016.
- [CTM⁺22] Y. Chew, T. Tomita, T. P. Mahesh, S. Sugawa, S. de Léséleuc, and K. Ohmori. Ultrafast energy exchange between two single rydberg atoms on a nanosecond timescale. *Nature Photonics*, 16(10):724–729, 2022.
- [DCS⁺23] Alexander M. Dalzell, B. David Clader, Grant Salton, Mario Berta, Cedric Yen-Yu Lin, David A. Bader, Nikitas Stamatopoulos, Martin J. A. Schuetz, Fernando G. S. L. Brandão, Helmut G. Katzgraber, and William J. Zeng. End-to-end resource analysis for quantum interior-point methods and portfolio optimization. *PRX Quantum*, 4:040325, Nov 2023.
- [DR59] George B. Dantzig and John H. Ramser. The truck dispatching problem. *Management science*, 6(1):80–91, 1959.
- [FSP16] Hamza Fawzi, James Saunderson, and Pablo A. Parrilo. Sparse sums of squares on finite abelian groups and improved semidefinite lifts. *Mathematical Programming*, 160(1):149–191, 2016.
- [FTB⁺18] Fabio Furini, Emiliano Traversi, Pietro Belotti, Antonio Frangioni, Ambros Gleixner, Nick Gould, Leo Liberti, Andrea Lodi, Ruth Misener, Hans Mittelmann, Nikolaos Sahinidis, Stefan Vigerske, and Angelika Wiegele. QPLIB: A library of quadratic programming instances. *Mathematical Programming Computation*, 2018.
- [GBKSF22] Fernando G.S.L. Brandão, Richard Kueng, and Daniel Stilck França. Faster quantum and classical SDP approximations for quadratic binary optimization. *Quantum*, 6:625, 2022.
- [GCG21] Michael Garstka, Mark Cannon, and Paul Goulart. COSMO: A conic operator splitting method for convex conic problems. *Journal of Optimization Theory and Applications*, 190(3):779–810, 2021.
- [GH20] Erica K. Grant and Travis S. Humble. Adiabatic quantum computing and quantum annealing, 2020.
- [GH22] Smitha Gopinath and Hassan L. Hijazi. Benchmarking large-scale acopf solutions and optimality bounds. In *2022 IEEE Power & Energy Society General Meeting (PESGM)*, pages 1–5, 2022.
- [GHL⁺22] Nicolò Gusmeroli, Timotej Hrga, Borut Lužar, Janez Povh, Melanie Siebenhofer, and Angelika Wiegele. Biqbin: A parallel branch-and-bound solver for binary quadratic problems with linear constraints. *ACM Trans. Math. Softw.*, 48(2), 2022.
- [GJS74] Michael R Garey, David S Johnson, and Larry Stockmeyer. Some simplified np-complete problems. In *Proceedings of the sixth annual ACM symposium on Theory of computing*, pages 47–63, 1974.
- [GK18] Fred W. Glover and Gary A. Kochenberger. A tutorial on formulating QUBO models. *CoRR*, abs/1811.11538, 2018.
- [GMM16] Bissan Ghaddar, Jakub Marecek, and Martin Mevissen. Optimal power flow as a polynomial optimization problem. *IEEE Transactions on Power Systems*, 31(1), 2016.
- [GRS24] Einar Gabbassov, Gili Rosenberg, and Artur Scherer. Lagrangian duality in quantum optimization: Overcoming qubo limitations for constrained problems, 2024.
- [Gur24] Gurobi Optimization, LLC. Gurobi Optimizer Reference Manual, 2024.
- [GW95] Michel X. Goemans and David P. Williamson. Improved approximation algorithms for maximum cut and satisfiability problems using semidefinite programming. *J. ACM*, 42(6):1115–1145, 1995.

- [Hel00] Keld Helsgaun. An effective implementation of the lin–kernighan traveling salesman heuristic. *European journal of operational research*, 126(1):106–130, 2000.
- [Hel17] Keld Helsgaun. An extension of the lin-kernighan-helsgaun tsp solver for constrained traveling salesman and vehicle routing problems. *Roskilde: Roskilde University*, 12:966–980, 2017.
- [HKS23] Soodeh Habibi, Michal Kočvara, and Michael Stingl. Solving Lasserre relaxations of unconstrained binary quadratic optimization problems by an interior-point method. working paper or preprint, 2023.
- [HKS24] Soodeh Habibi, Michal Kočvara, and Michael Stingl. Loraine – an interior-point solver for low-rank semidefinite programming. *Optimization Methods and Software*, 39(6):1185–1215, 2024.
- [HL03] Didier Henrion and Jean-Bernard Lasserre. Gloptipoly: Global optimization over polynomials with matlab and sedumi. *ACM Trans. Math. Softw.*, 29(2):165–194, 2003.
- [HL05] Didier Henrion and Jean-Bernard Lasserre. *Detecting Global Optimality and Extracting Solutions in GloptiPoly*, volume 312, pages 581–581. 2005.
- [HP21] Timotej Hrga and Janez Povh. Madam: a parallel exact solver for max-cut based on semidefinite programming and admm. *Computational Optimization and Applications*, 80(2):347–375, 2021.
- [HTO⁺25] Fabian Henze, Viet Tran, Birte Ostermann, Richard Kueng, Timo de Wolff, and David Gross. Solving quadratic binary optimization problems using quantum sdp methods: Non-asymptotic running time analysis, 2025.
- [HXL⁺23] Tian Huang, Jun Xu, Tao Luo, Xiaozhe Gu, Rick Goh, and Weng-Fai Wong. Benchmarking quantum(-inspired) annealing hardware on practical use cases. *IEEE Transactions on Computers*, 72(6):1692–1705, 2023.
- [IdW16] Sadik Iliman and Timo de Wolff. Amoebas, nonnegative polynomials and sums of squares supported on circuits. *Res. Math. Sci.*, 3:3:9, 2016.
- [Jac01] Paul Jaccard. Distribution de la flore alpine dans le bassin des dranses et dans quelques régions voisines. *Bull Soc Vaudoise Sci Nat*, 37:241–272, 1901.
- [JLM⁺21] Michael Jünger, Elisabeth Lobe, Petra Mutzel, Gerhard Reinelt, Franz Rendl, Giovanni Rinaldi, and Tobias Stollenwerk. Quantum annealing versus digital computing: An experimental comparison. *ACM J. Exp. Algorithmics*, 26, 2021.
- [JLN⁺10] Michael Jünger, Thomas M. Lieblich, Denis Naddef, George L. Nemhauser, William R. Pulleyblank, Gerhard Reinelt, Giovanni Rinaldi, and Laurence A. Wolsey, editors. *50 Years of Integer Programming 1958-2008: From the Early Years to the State-of-the-Art*. Springer, Berlin, Heidelberg, 2010.
- [KBPV22] Thorsten Koch, Timo Berthold, Jaap Pedersen, and Charlie Vanaret. Progress in mathematical programming solvers from 2001 to 2020. *EURO Journal on Computational Optimization*, 10:100031, 2022.
- [KHG⁺14] Gary Kochenberger, Jin-Kao Hao, Fred Glover, Mark Lewis, Zhipeng Lü, Haibo Wang, and Yang Wang. The unconstrained binary quadratic programming problem: a survey. *J. Comb. Optim.*, 28(1):58–81, 2014.
- [KMR17] Nathan Krislock, Jérôme Malick, and Frédéric Roupin. Biqcrunch: A semidefinite branch-and-bound method for solving binary quadratic problems. *ACM Trans. Math. Softw.*, 43(4), 2017.
- [Kof15] Monika Kofler. *Optimising the storage location assignment problem under dynamic conditions*. PhD thesis, Johannes Kepler University Linz, 2015.
- [Las01] Jean-Bernard Lasserre. Global optimization with polynomials and the problem of moments. *SIAM Journal on Optimization*, 11(3):796–817, 2001.
- [Las15] Jean-Bernard Lasserre. *An Introduction to Polynomial and Semi-Algebraic Optimization*, volume 1 of *Cambridge Texts in Applied Mathematics*. Cambridge University Press, Cambridge, United Kingdom, 2015.
- [Lau03] Monique Laurent. Lower bound for the number of iterations in semidefinite hierarchies for the cut polytope. *Mathematics of Operations Research*, 28(4):871–883, 2003.
- [Lau09] Monique Laurent. Sums of squares, moment matrices and optimization over polynomials. In *Emerging applications of algebraic geometry*, volume 149 of *IMA Vol. Math. Appl.*, pages 157–270. Springer, New York, 2009.
- [LCD⁺17] Benoît Legat, Chris Coey, Robin Deits, Joey Huchette, and Amelia Perry. Sum-of-squares optimization in Julia. In *The First Annual JuMP-dev Workshop*, 2017.

- [LCY20] In Gyu Lee, Sung Hoon Chung, and Sang Won Yoon. Two-stage storage assignment to minimize travel time and congestion for warehouse order picking operations. *Computers & Industrial Engineering*, 139:106129, 2020.
- [LM04] Chi-Guhn Lee and Zhong Ma. The generalized quadratic assignment problem. *Research Rep., Dept., Mechanical Industrial Eng., Univ. Toronto, Canada*, page M5S, 2004.
- [LMMT⁺21] Yue Li, Francis A. Méndez-Mediavilla, Cecilia Temponi, Junwoo Kim, and Jesus A. Jimenez. A heuristic storage location assignment based on frequent itemset classes to improve order picking operations. *Applied Sciences*, 11(4), 2021.
- [LMN16] Jiaxi Li, Mohsen Moghaddam, and Shimon Nof. Dynamic storage assignment with product affinity and abc classification—a case study. *The International Journal of Advanced Manufacturing Technology*, 2016.
- [Mit24] Hans D. Mittelmann. Decision tree for optimization software. <https://plato.asu.edu/guide.html>, 2024. Accessed 02/25.
- [MTZ60] Clair E Miller, Albert W Tucker, and Richard A Zemlin. Integer programming formulation of traveling salesman problems. *Journal of the ACM (JACM)*, 7(4):326–329, 1960.
- [MW21] Victor Magron and Jie Wang. TSSOS: a Julia library to exploit sparsity for large-scale polynomial optimization. <https://arxiv.org/abs/2103.00915>, 2021.
- [MW23] Renee Mirka and David P. Williamson. An experimental evaluation of semidefinite programming and spectral algorithms for max cut. *ACM J. Exp. Algorithmics*, 28, 2023.
- [Now24] Julian Nowak. Solving the storage location assignment problem using affinity-based slotting. *Master’s Thesis, Technische Universität Dortmund*, 2024.
- [OCPB23] Brendan O’Donoghue, Eric Chu, Neal Parikh, and Stephen Boyd. SCS: Splitting conic solver, version 3.2.7. <https://github.com/cvxgrp/scs>, 2023.
- [OUN⁺17] Ryosuke Okuta, Yuya Unno, Daisuke Nishino, Shohei Hido, and Crissman Loomis. Cupy: A numpy-compatible library for nvidia gpu calculations. In *Proceedings of Workshop on Machine Learning Systems (LearningSys) in The Thirty-first Annual Conference on Neural Information Processing Systems (NIPS)*, 2017.
- [Par00] Pablo A. Parrilo. *Structured semidefinite programs and semialgebraic geometry methods in robustness and optimization*. California Institute of Technology, 2000.
- [Put93] Mihai Putinar. Positive polynomials on compact semi-algebraic sets. *Indiana University Mathematics Journal*, 42(3):969–984, 1993.
- [RKS23] Daniel Rehfeldt, Thorsten Koch, and Yuji Shinano. Faster exact solution of sparse maxcut and qubo problems. *Mathematical Programming Computation*, 15(3):445–470, 2023.
- [RP06] Stefan Ropke and David Pisinger. An adaptive large neighborhood search heuristic for the pickup and delivery problem with time windows. *Transportation Science*, 40(4), 2006.
- [RRW10] Franz Rendl, Giovanni Rinaldi, and Angelika Wiegele. Solving Max-Cut to optimality by intersecting semidefinite and polyhedral relaxations. *Math. Programming*, 121(2):307, 2010.
- [SA90] Hanif D. Sherali and Warren P. Adams. A hierarchy of relaxations between the continuous and convex hull representations for zero-one programming problems. *SIAM Journal on Discrete Mathematics*, 3(3):411–430, 1990.
- [STKI17] Shinsaku Sakaue, Akiko Takeda, Sunyoung Kim, and Naoki Ito. Exact semidefinite programming relaxations with truncated moment matrix for binary polynomial optimization problems. *SIAM Journal on Optimization*, 27(1):565–582, 2017.
- [SWW21] Stefan Sremac, Hugo J. Woerdeman, and Henry Wolkowicz. Error bounds and singularity degree in semidefinite programming. 31(1), 2021.
- [Sys] D-Wave Systems. Leap: The quantum cloud service. <https://www.dwavesys.com/solutions-and-products/cloud-platform>. Accessed: 01/25.
- [TGGP01] E. Taillard, L. Gambardella, M. Gendreau, and J. Potvin. Adaptive memory programming: A unified view of metaheuristics. *European Journal of Operational Research*, 135:1–16, 2001.
- [The24] Thorsten Theobald. *Real algebraic geometry and optimization*, volume 241 of *Graduate Studies in Mathematics*. American Mathematical Society, Providence, RI, 2024.
- [TV02] Paolo Toth and Daniele Vigo. *The vehicle routing problem*. SIAM, 2002.
- [vAG19] Joran van Apeldoorn and Andrés Gilyén. Improvements in Quantum SDP-Solving with Applications. pages 99:1–99:15. Schloss Dagstuhl – Leibniz-Zentrum für Informatik, 2019.

- [vAGGdW20] Joran van Apeldoorn, András Gilyén, Sander Gribling, and Ronald de Wolf. Quantum SDP-Solvers: Better upper and lower bounds. *Quantum*, 4:230, 2020.
- [WH24] Jie Wang and Liangbing Hu. Solving low-rank semidefinite programs via manifold optimization, 2024.
- [Wie07] Angelika Wiegele. Biq mac library - a collection of max-cut and quadratic 0-1 programming instances of medium size, 2007.
- [WJW21] Yun Dong Wei Jiang, Jiyin Liu and Li Wang. Assignment of duplicate storage locations in distribution centres to minimise walking distance in order picking. *International Journal of Production Research*, 59(15):4457–4471, 2021.
- [WKK⁺08] Hayato Waki, Sunyoung Kim, Masakazu Kojima, Masakazu Muramatsu, and Hiroshi Sugimoto. Algorithm 883: Sparsepop—a sparse semidefinite programming relaxation of polynomial optimization problems. *ACM Trans. Math. Softw.*, 35(2), 2008.
- [WLC⁺19] Tillmann Weisser, Benoît Legat, Chris Coey, Lea Kapelevich, and Juan Pablo Vielma. Polynomial and moment optimization in julia and jump. In *JuliaCon*, 2019.
- [WML19] Jie Wang, Victor Magron, and Jean-Bernard Lasserre. TSSOS. <https://github.com/wangjie212/TSSOS>, 2019. MIT license, accessed 02/24.
- [WML20a] Jie Wang, Victor Magron, and Jean-Bernard Lasserre. Chordal-tssos: a moment-sos hierarchy that exploits term sparsity with chordal extension. <https://arxiv.org/abs/2005.02828>, 2020.
- [WML20b] Jie Wang, Victor Magron, and Jean-Bernard Lasserre. Tssos: A moment-sos hierarchy that exploits term sparsity. <https://arxiv.org/abs/1912.08899>, 2020.
- [WMLM21] Jie Wang, Victor Magron, Jean-Bernard Lasserre, and Ngoc Hoang Anh Mai. CS-TSSOS: Correlative and term sparsity for large-scale polynomial optimization. <https://arxiv.org/abs/2005.02828>, 2021.
- [YJR16] Vincent F. Yu, Parida Jewpanya, and A.A.N. Perwira Redi Redi. Open vehicle routing problem with cross-docking. *Computers & Industrial Engineering*, 94:6–17, 2016.

APPENDIX A. TECHNICAL DETAILS IN PROBLEM FORMULATIONS

A.1. Affinity Matrix in ASP. We provide the definition of the ASP in (3.10). In this section, we give additional details for the affinity measure. We have that \mathcal{M} is the set of material types and $\sigma \in \mathbb{R}^{|\mathcal{M}| \times |\mathcal{M}|}$ is a real, symmetric matrix with positive entries and zeros on the diagonal, which determines the affinity σ_{mn} for every pair of materials m and n in \mathcal{M} . More specifically,

$$\sigma = \frac{O_{mn}}{\delta_m + \delta_n - O_{mn}},$$

where $O \in \mathbb{R}_{\geq 0}^{|\mathcal{M}| \times |\mathcal{M}|}$ is a symmetric matrix with zeros on the diagonal and $\delta_m \in \mathbb{Z}_{\geq 0}$. The number O_{mn} is the number of times the materials m and n appear together in an order and δ_m is the total number of orders in which m appears. Therefore $\delta_m + \delta_n > O_{mn}$ for all $m, n \in \mathcal{M}$ – otherwise the problem in Eq. (3.10) is degenerate.

A.2. QUBO Reformulation. Below, we demonstrate the process of converting the IQP formulation of an ASP to its QUBO formulation. We exemplarily consider the smallest ASP instance ASP30 with 30 materials and three aisles with a capacity of ten storage locations. For the QUBO reformulation we follow the methodology developed by Glover et al. [GK18].

A.2.1. Unconstraining. Consider the IQP model of the ASP in (3.10). In this step, we incorporate the constraints into the objective function. We can include the equality constraints (3.11) directly, while inequality constraints (3.12) require slack variables to convert them into equalities before incorporation. For each aisle A_j with $j = 1, \dots, k$ we introduce a *slack variable*

s_j in $\mathbb{Z}_{\geq 0}$. Moreover, let $\lambda \in \mathbb{Z}$ be the *scalar penalization factor*. We rewrite the IQP (3.10) as

$$\begin{aligned}
\text{(A.1)} \quad \min \quad & \sum_{m,n \in \mathcal{M}} \sum_{\substack{i,j=1 \\ i \neq j}}^k \sigma_{mn} x_{mi} x_{nj} + \lambda \sum_{m \in \mathcal{M}} \left(\sum_{j=1}^k x_{mj} - 1 \right)^2 \\
& + \lambda \sum_{j=1}^k \left(\sum_{m \in \mathcal{M}} x_{mj} + s_j - |A_j| \right)^2 \\
\text{subject to} \quad & x_{mj} \in \{0, 1\}, & \text{for all } m \in \mathcal{M}, \\
& & \text{and } j = 1, \dots, k \\
& 0 \leq s_j \leq |A_j|, & \text{for all } j = 1, \dots, k.
\end{aligned}$$

Note that it is possible to introduce an integer slack variable s_j for $j = 1, \dots, k$ since, in the inequality constraint (3.12), the summand on the left, as well as the aisle capacity $|A_j|$ on the right, are integers. The scalar penalization factor λ aims to ensure that the original constraints are satisfied, see Appendix A.2.3 for details. Note that the quadratic penalty terms in the objective function in (A.1) amplify larger deviations when the constraints are violated.

Now, in the example of ASP30, since the number of aisles is three, the total number of integer slack variables is also three.

A.2.2. Binarization. The above step removes the constraints (3.11) and (3.12) from the original ASP formulation and introduces integer variables $s_j \in \mathbb{Z}_{\geq 0}$, for $j = 1, \dots, k$, where k is the number of aisles. In this step, we encode each of the integer slack variables with binary variables.

Recall, that $|A_j|$ is the aisle capacity of an aisle A_j . In what follows, let $r = \lfloor \log_2(|A_j|) \rfloor$. For each aisle A_j with $j = 1, \dots, k$, we define the corresponding slack variable as

$$\text{(A.2)} \quad s_j = \sum_{s=1}^{r+1} c_s^{(j)} y_s^{(j)},$$

via introducing (for $s = 1, \dots, r+1$) *auxiliary binary variables* $y_s^{(j)} \in \{0, 1\}$ and *coefficients* $c_s^{(j)} \in \mathbb{N}$. Furthermore, we can define the coefficients $c_s^{(j)}$, for all $s = 1, \dots, r+1$ and $j = 1, \dots, k$ in detail via

$$c_s^{(j)} = \begin{cases} 2^{s-1}, & \text{if } s = 1, \dots, r \\ |A_j| - (2^r - 1), & \text{if } s = r + 1. \end{cases}$$

In the example of ASP30, we have $|A_j| = 10$ for $j = 1, 2, 3$, since we have three aisles with ten storage locations per aisle. This requires a total of four binary variables for each aisle, leading to a total of 12 auxiliary binary variables.

With the definition in (A.2), we replace the slack variables in (A.1). This leads to

$$\begin{aligned}
 \text{(A.3)} \quad \min \quad & \sum_{m,n \in \mathcal{M}} \sum_{\substack{i,j=1 \\ i \neq j}}^k \sigma_{mn} x_{mi} x_{nj} + \lambda \sum_{m \in \mathcal{M}} \left(\sum_{j=1}^k x_{mj} - 1 \right)^2 \\
 & + \lambda \sum_{j=1}^k \left(\sum_{m \in \mathcal{M}} x_{mj} + \sum_{s=1}^{r+1} c_s^{(j)} y_s^{(j)} - |A_j| \right)^2 \\
 \text{subject to} \quad & x_{mj} \in \{0, 1\}, & \text{for all } m \in \mathcal{M}, \\
 & & \text{and } j = 1, \dots, k \\
 & y_s^{(j)} \in \{0, 1\}, & \text{for all } s = 1, \dots, r+1, \\
 & & \text{and } j = 1, \dots, k.
 \end{aligned}$$

Finally, we reach the QUBO formulation in (2.1), via expanding quadratic penalty terms and omitting the constant term, which does not affect optimization.

Considering the example ASP30, we reformulate the original problem (3.10) as a QUBO with 96 binary variables. These consists of 12 auxiliary binary variables and 84 for the assignment of each material $m \in \mathcal{M}$ to an aisle A_j with $j = 1, \dots, k$. Since two materials $m, n \in \mathcal{M}$ have affinity $\sigma_{mn} = 0$, the binary variables reduce from 90 to 84.

Note that, as we demonstrate in this subsection, the number of binary variables required to reformulate an IQP, and similarly an IP, into a QUBO grows logarithmically with the upper bound of the slack variables, which in this case is the aisle capacity of each aisle.

A.2.3. Penalization. It is nontrivial to select the appropriate penalization factor $\lambda \in \mathbb{Z}$ in (A.1), respectively (A.3), for the reformulation. However, knowledge about the range of the objective function value can be very useful in this regard. As explained in [GK18] and [KHG⁺14], there is a ‘‘Goldilocks region’’ where penalty values strike a balance and work effectively. This region is typically broad, offering some flexibility. To estimate an appropriate penalization factor, a preliminary analysis of the original model can help provide a rough approximation of the objective function’s value. A good starting point is to set the penalty between 75% and 150% of this estimate, then iteratively adjust based on feasibility until an acceptable solution is found.

APPENDIX B. FURTHER CERTIFICATES OF NONNEGATIVITY BEYOND SOS-SDP

As pointed out, QUBOs fall into the broader range of polynomial optimization problems (on the boolean hypercube). There exist various other certificates of nonnegativity beyond SOS that are tractable via convex optimization problems. These include for example *sums of nonnegative circuit polynomials (SONC)* certificates, which are also referred to *sums of AM/GM exponentials (SAGE)*, which can be computed via relative entropy programs; see e.g., [IdW16, CS16]. On the boolean hypercube, another prominent hierarchy is the Sherali-Adams hierarchy, which leads to a linear programming formulation [SA90]. Furthermore, recently a new certificate named *sums of copositive fewnomials* was suggested [AS25]. We decided against including these certificates in the experimental comparison carried out in this work first due to the complexity of the endeavor, second since at least in some of the cases proper implementations are not available, and third since we aim to focus on a comparison of SDP-based methods with Hamiltonian Updates.

Finally, a very natural certificate to consider here would be *scaled diagonally dominant sum of squares (SDSOS)*, which are tractable by SOCPs [AM19]. SDSOS are hence a special case

of SOS, which are, however, easier to compute (they happen moreover to be SONCs). Unfortunately, as it was confirmed to us by one of the developers, no implementation suitable for the experiments carried out in this paper is available at the moment.

APPENDIX C. CONVERTING QUBOS TO ISING FORMULATION

We convert our initial QUBO problem $\min_{\mathbf{b}} \mathbf{b}^T Q \mathbf{b}$, with $\mathbf{b} \in \{0, 1\}^n$ and $Q \in \mathbb{R}^{n \times n}$, see (2.1), to $\min_{\mathbf{x}} \mathbf{x}^T C \mathbf{x}$ with $\mathbf{x} \in \{-1, 1\}^{n+1}$ and $C \in \mathbb{R}^{(n+1) \times (n+1)}$. This formulation is also known as the *Ising formulation* used for Hamiltonian Updates, see (5.1), as well as an alternative input for the polynomial optimization software. In order to construct C , we insert an additional variable x_0 that we constrain to be $x_0 = 1$. We convert between the vectors \mathbf{b} and \mathbf{x} via $b_i = (x_i + 1)/2$ for all $i = 1, \dots, n$. The new polynomial $f(1, \mathbf{x})$ given by the new cost matrix $C \in \mathbb{R}^{(n+1) \times (n+1)}$ looks as follows. Recall that Q is a symmetric matrix. Thus, we have

$$\begin{aligned} f(1, \mathbf{x}) &= [1, \mathbf{x}]^T C [1, \mathbf{x}] \\ &= [1 \quad x_1 \quad x_2 \quad \dots \quad x_n] \frac{1}{4} \left[\begin{array}{c|ccc} \sum_{i,j=1}^n q_{ij} & \sum_{i=1}^n q_{i1} & \dots & \sum_{i=1}^n q_{in} \\ \hline \sum_{i=1}^n q_{i1} & q_{11} & \dots & q_{1n} \\ \vdots & \vdots & \ddots & \vdots \\ \sum_{i=1}^n q_{in} & q_{1n} & \dots & q_{nn} \end{array} \right] \begin{bmatrix} 1 \\ x_1 \\ x_2 \\ \vdots \\ x_n \end{bmatrix} \\ &= \frac{1}{4} \left(\mathbf{x}^T Q \mathbf{x} + 2 \sum_{j=1}^n x_j \sum_{i=1}^n q_{ij} + \sum_{i,j}^n q_{ij} \right). \end{aligned}$$

The advantage of using $\{-1, 1\}$ as binary representation instead of $\{0, 1\}$ is that all monomials of the form $q_{ii}x_i^2$ become directly constant, i.e., $q_{ii}x_i^2 = q_{ii}$ for $x_i = \pm 1$. This directly reduces the number of monomials, in particular all n monomials corresponding to the diagonal of C are now constant.

APPENDIX D. TECHNICAL DETAILS IN SDP RELAXATIONS

D.1. Time Limits. In Table 11 we display the time limits we enforce for the SDP relaxations. For a single parameter choice, we give a time limit of the number of instances in each set times one hour for ASP instances, and times two hours for OVRP instances. For example, since there are 14 QUBOs corresponding to ASP30, we enforce a time limit of 14 hours for one run with a specific parameter set through all ASP30 instances. Exemplarily, we rerun and provide outcomes of computations that were exceeding the initial time limit.

Instance Set	ASP30	ASP60	ASP90	OVRP
Time Limit in hours	14	4	3	4

TABLE 11. Imposed **time limits** in hours for one run through the entire set of instances with each parameter choice.

D.2. SOS Solver Settings. For the SDP solvers inside TSSOS [MW21], we test different tolerances in the solver settings in order to achieve solutions with higher/lower precision:

- For MOSEK [ApS24], we set *primal feasibility tolerance*, *dual feasibility tolerance*, as well as *primal-dual gap tolerance* to $\{10^{-8}, 10^{-4}\}$ and refer to default parameters as set up in the documentation of [WML19].
- For COSMO [GCG21], we set *absolute residual tolerance* and *relative residual tolerance* to $\{10^{-5}, 10^{-3}\}$ and refer to default parameters as set up in the documentation of [WML19].

Using the MANISDP solver directly for the moment version of (4.4), we use the default parameters for SDPs with diagonal and unit-diagonal constraints respectively, as given in the documentation of [WH24]. For SOS.JL, we use the default settings of MOSEK [ApS24] and LORAINE [HKS24]. We also use the default settings for the solver SCS [OCPB23].

APPENDIX E. ADDITIONAL DATA

In the additional tables we provide information about the absolute differences $\Delta_{\text{QUBO}}^{\text{abs}}$, $\Delta_{\text{SOS}}^{\text{abs}}$, $\Delta_{\text{HU}}^{\text{abs}}$ to the optimal values, as well as $\tilde{\Delta}_{\text{HU}}^{\text{abs}}$, $\tilde{\Delta}_{\text{HU}}^{\text{rel}}$ for the upper bounds achieved via the randomized rounding procedure in HU. For reference, the optimal values are $Z^* \approx 246.78$ for ASP30, $Z^* \approx 820.08$ for ASP60 and $Z^* \approx 1373.15$ for ASP90, $Z^* \approx 6254.19$ for OVRP11 and $Z^* \approx 3036.54$ for OVRP15, see Table 4.

E.1. SOS-SDP. In addition to Table 8, we give the **average** of the **absolute difference** $\Delta_{\text{SOS}}^{\text{abs}}$ of the lower bound Z_{SOS} to the optimal value using SOS-SDP methods for the ASP instances in Table 12.

	ASP30		ASP60		ASP90	
	Average $\Delta_{\text{SOS}}^{\text{abs}}$	Average t_{SOS}	Average $\Delta_{\text{SOS}}^{\text{abs}}$	Average t_{SOS}	Average $\Delta_{\text{SOS}}^{\text{abs}}$	Average t_{SOS}
MANISDP	491.1	1.45s	2468.6	0.82s	3308.6	1.45s
SOS.JL w. MOSEK	491.1	9.9s	2468.6	221.25s	3308.5	8256.9s
SOS.JL w. Loraine	491.1	670.66s	†	†	†	†
TSSOS w. MOSEK	491.1	3.24s	2468.6	112.42s	†	†
TSSOS w. MOSEK	32.72	28.46s	174.3	912.47s	†	†

TABLE 12. **Results of SOS-SDP relaxations** of QUBOs referring to ASP30, ASP60 and ASP90. We display the **average** of the **absolute difference** $\Delta_{\text{SOS}}^{\text{abs}}$ of the lower bound Z_{SOS} to the optimal value. The gray row refers to the second order Lasserre relaxation, the other rows refer to the first order relaxation. A dagger '†' indicates that no result is available due to solver break down or exceeding maximal running time. For MOSEK, we display the result with the default tolerance $\text{tol}=10^{-8}$. For SOS.JL with MOSEK the total solving time of all ASP90 instances exceeds our set time limit. We display a rerun for these instances without time limit.

E.2. HU. In addition to Tables 7 and 10, we show the **absolute difference** of the **lower bound** $\Delta_{\text{HU}}^{\text{abs}}$ to Z^* , and the absolute and relative differences of the **upper bound** $\tilde{\Delta}_{\text{HU}}^{\text{abs}}$ and $\tilde{\Delta}_{\text{HU}}^{\text{rel}}$ for OVRP, as well as selected ASP instances, using HU in Tables 13 and 14, respectively.

	OVRP11			OVRP15		
	$\Delta_{\text{HU}}^{\text{abs}}$	$\tilde{\Delta}_{\text{HU}}^{\text{abs}}$	$\tilde{\Delta}_{\text{HU}}^{\text{rel}}$	$\Delta_{\text{HU}}^{\text{abs}}$	$\tilde{\Delta}_{\text{HU}}^{\text{abs}}$	$\tilde{\Delta}_{\text{HU}}^{\text{rel}}$
$\text{HU}^*_{\epsilon = 10^{-2}}$	5.0×10^{10}	1.4×10^9	2.1×10^5	1.7×10^{12}	2.5×10^9	8.4×10^5
$\text{HU}^*_{\epsilon = 10^{-3}}$	4.7×10^9	1.3×10^9	2.1×10^5	1.9×10^{10}	2.6×10^9	8.5×10^5
$\text{HU}^*_{\epsilon = 10^{-4}}$	4.4×10^8	3.7×10^7	5.9×10^3	1.7×10^9	6.7×10^7	2.2×10^4

TABLE 13. **Results of SDP relaxations via HU** of QUBOs referring to OVRP11 and OVRP15 on **GPU**. We display the absolute difference of the **lower bound** $\Delta_{\text{HU}}^{\text{abs}}$ to Z^* , and the absolute and relative differences of the **upper bound** $\tilde{\Delta}_{\text{HU}}^{\text{abs}}$ and $\tilde{\Delta}_{\text{HU}}^{\text{rel}}$. The '*' indicates that the results are obtained via GPU.

	ASP60-850			ASP90-1400		
	$\Delta_{\text{HU}}^{\text{abs}}$	$\tilde{\Delta}_{\text{HU}}^{\text{abs}}$	$\tilde{\Delta}_{\text{HU}}^{\text{rel}}$	$\Delta_{\text{HU}}^{\text{abs}}$	$\tilde{\Delta}_{\text{HU}}^{\text{abs}}$	$\tilde{\Delta}_{\text{HU}}^{\text{rel}}$
$\text{HU}^*_{\epsilon = 10^{-2}}$	4.4×10^6	1.4×10^5	172.3	2.7×10^7	5.3×10^5	386.1
$\text{HU}^*_{\epsilon = 10^{-3}}$	6.6×10^5	2.9×10^4	35.9	3.7×10^6	7.7×10^4	55.8
$\text{HU}^*_{\epsilon = 10^{-4}}$	6.1×10^4	1.3×10^4	15.9	3.5×10^5	3.6×10^4	25.9

TABLE 14. **Results of SDP relaxations via HU** of QUBOs referring to ASP60-850 and ASP90-1400. We display the absolute difference of the **lower bound** $\Delta_{\text{HU}}^{\text{abs}}$ to Z^* , and the absolute and relative differences of the **upper bound** $\tilde{\Delta}_{\text{HU}}^{\text{abs}}$ and $\tilde{\Delta}_{\text{HU}}^{\text{rel}}$. The '*' indicates that the results are obtained via GPU.

E.3. **QUBO Solver Results.** In addition to Table 5, in Table 15 we display the **absolute difference** $\Delta_{\text{QUBO}}^{\text{abs}}$ to the optimal value Z^* , solving the QUBO formulation with GUROBI.

Instance	Time Limit	$\Delta_{\text{QUBO}}^{\text{abs}}$	Time Limit	$\Delta_{\text{QUBO}}^{\text{abs}}$	Time Limit	$\Delta_{\text{QUBO}}^{\text{abs}}$
ASP30-950	10s	0	120s	0	600s	0
ASP60-900	10s	240.3	120s	240.3	600s	240.3
ASP90-1450	10s	1020.6	120s	270.9	600s	262.9

TABLE 15. **Absolute difference** $\Delta_{\text{QUBO}}^{\text{abs}}$ of the **upper bound** Z_{QUBO} to the optimal value Z^* for selected **QUBOs** using GUROBI with different time limits. For ASP30-950 we find the optimal value. The provided time limits are upper bounds on the running time to reach the respective objective value Z_{QUBO} . The computation is stopped at the provided time limit.

E.4. **Additional Quantum Annealer Results.** In addition to Subsection 6.2.1 and Table 15, where we solve the QUBO formulations via the classic and commercial solvers CPLEX and GUROBI, we exemplarily give an overview on solving them via the quantum annealer from D-Wave [Sys], using the QUBO_SOLVE tool from GAMS, see Subsection 6.1. We emphasize, that quantum annealing is not the main focus of our study, we provide these results for reference. Moreover, we point out, that these results are not easily reproducible as the free developer access is no longer available. We see in Table 16 that, similar to solving via the classical solvers, we find feasible solutions for the ASP instances, but the solutions for the OVRP instances are infeasible.

Instance	ASP30-450	ASP60-900	ASP90-1450	OVRP11	OVRP15
$\Delta_{\text{QUBO}}^{\text{abs}}$	0	65.4	843.4	infeasible	infeasible
$\Delta_{\text{QUBO}}^{\text{rel}}$	0	0.08	0.61	infeasible	infeasible
Time Limit	120s	120s	120s	60s	60s

TABLE 16. **Absolute difference** $\Delta_{\text{QUBO}}^{\text{abs}}$ and **relative difference** $\Delta_{\text{QUBO}}^{\text{rel}}$ of the **upper bound** Z_{QUBO} to the optimal value Z^* for selected **QUBOs** using **quantum annealing** by D-Wave with indicated time limits. For ASP30-450 we find the optimal value. We stop the computation at the given time limit. Note that we also find the optimal value for ASP30-450 for a time limit of 30s and 60s.